REPORT

OPEN ACCESS

A phenotype-independent "label-capture-release" process for isolating viable circulating tumor cells in real-time drug susceptibility testing

Zhiqi Lao,[1,6] Xiaoxue Ren,[1,6] Dehua Zhuang,[2] Lingxia Xie,[1] Yucong Zhang,[2] Wei Li,[1,*] Yue Chen,[2,*] Penghui Li,[1] Liping Tong,[1] Paul K. Chu,[3] and Huaiyu Wang[1,4,5,*]

*Correspondence: wei.li@siat.ac.cn (W.L.); chenyue_dr@163.com (Y.C.); hy.wang1@siat.ac.cn (H.W.)

Received: November 5, 2024; Accepted: January 10, 2025; Published Online: May 5, 2025; https://doi.org/10.1016/j.xinn.2025.100805

GRAPHICAL ABSTRACT

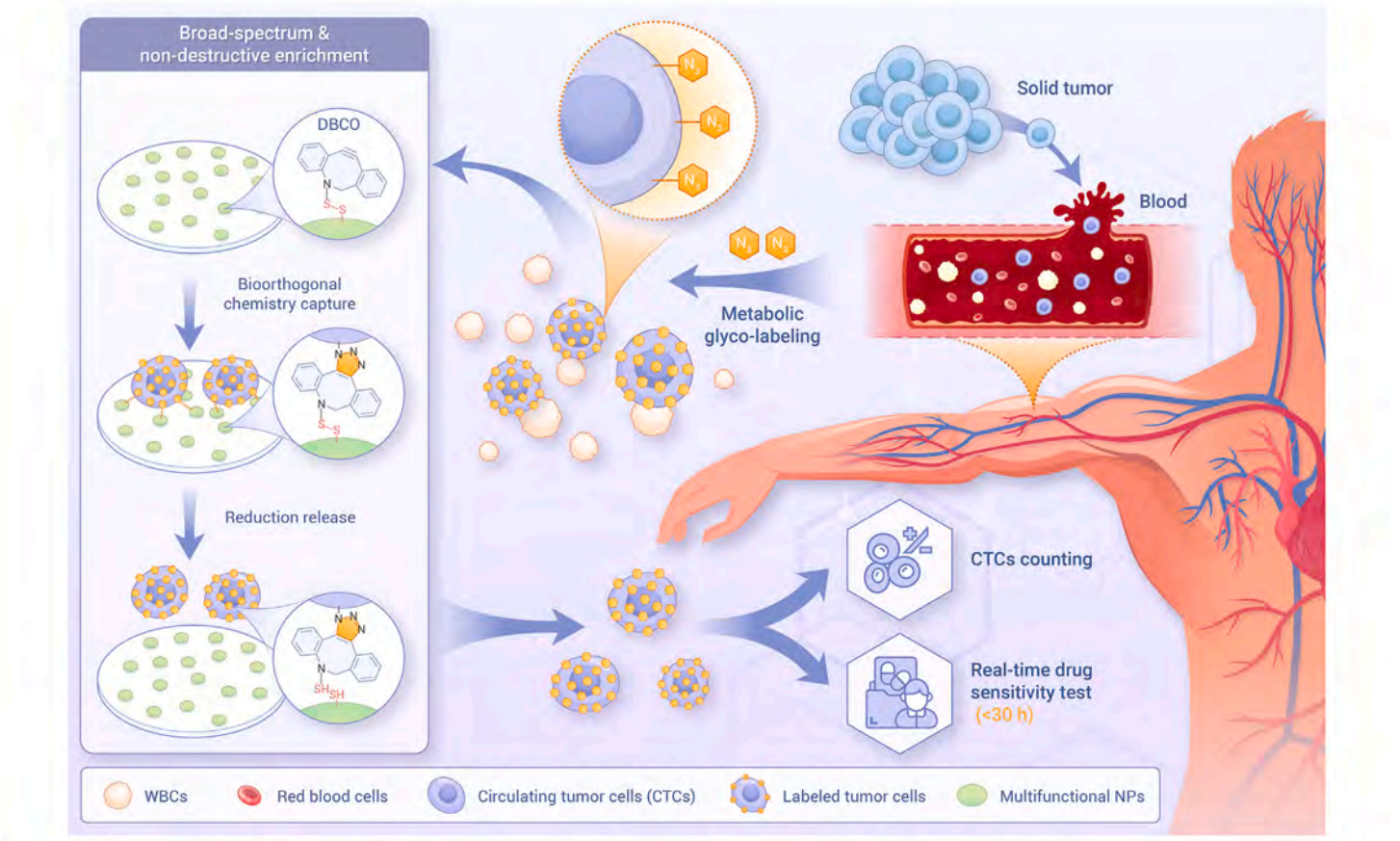

PUBLIC SUMMARY

- A label-capture-release workflow for precise circulating tumor cell (CTC) detection was developed.
- Metabolic glyco-labeling, click reaction, and disulfide reduction constituted the whole workflow.
- This method has shown feasibility in pan-cancer detection involving 10 kinds of clinical cancers.
- A novel real-time drug sensitivity test model for CTC downstream applications was also developed.

OPEN ACCESS

REPORT

The Innovation

A phenotype-independent "label-capture-release" process for isolating viable circulating tumor cells in real-time drug susceptibility testing

Zhiqi Lao,[1,6] Xiaoxue Ren,[1,6] Dehua Zhuang,[2] Lingxia Xie,[1] Yucong Zhang,[2] Wei Li,[1,*] Yue Chen,[2,*] Penghui Li,[1] Liping Tong,[1] Paul K. Chu,[3] and Huaiyu Wang[1,4,5,*]

[1]Institute of Biomedicine and Biotechnology, Shenzhen Institutes of Advanced Technology, Chinese Academy of Sciences, Shenzhen 518055, China

[2]Department of Medical Laboratory, Shenzhen People's Hospital (The Second Clinical Medical College, Jinan University, The First Affiliated Hospital, Southern University of Science and Technology), Shenzhen 518020, China

[3]Departments of Physics, Materials Science and Engineering, and Biomedical Engineering, City University of Hong Kong, Hong Kong SAR 999077, China

[4]Key Laboratory of Biomedical Imaging Science and System, Chinese Academy of Sciences, Shenzhen 518055, China

[5]State Key Laboratory of Biomedical Imaging Science and System, Shenzhen 518055, China

[6]These authors contributed equally

*Correspondence: wei.li@siat.ac.cn (W.L.); chenyue_dr@163.com (Y.C.); hy.wang1@siat.ac.cn (H.W.)

Received: November 5, 2024; Accepted: January 10, 2025; Published Online: May 5, 2025; https://doi.org/10.1016/j.xinn.2025.100805

Citation: Lao Z., Ren X., Zhuang D., et al., (2025). A phenotype-independent "label-capture-release" process for isolating viable circulating tumor cells in real-time drug susceptibility testing. The Innovation **6(5)**, 100805.

Although various strategies have been proposed for enrichment of circulating tumor cells (CTCs), the clinical outcomes of CTC detection are far from satisfactory. The prevailing methodologies for CTC detection are generally oriented toward naturally occurring targets; however, misdetection and interference are prevalent due to the diverse phenotypes and subpopulations of CTCs, which are highly heterogeneous. Here, a CTC isolation system based on the "label-capture-release" process is demonstrated for the precise and highly efficient enrichment of CTCs from clinical blood samples. On the basis of the abnormal glycometabolism of tumor cells, the surface of CTCs can be decorated with artificial azido groups. By utilizing bio-orthogonal plates designed with dibenzocyclooctane (DBCO) and disulfide groups, with the aid of anti-fouling effects, CTCs labeled with azido groups can be captured through a copper-free click reaction and subsequently released via disulfide reduction. The technique has been shown to label tumor cells with the epithelial cell adhesion molecule (EpCAM)+ and EpCAM− phenotypes in both adherent and suspended states. Moreover, it effectively isolates all epithelial, interstitial, and hybrid phenotypes of CTCs from clinical blood samples collected from dozens of patients across more than 10 cancer types. Compared to the clinically approved CTC detection system, our strategy demonstrates superior performance from the perspective of broad-spectrum and accurate recognition of heterogeneous CTCs. More importantly, most of the captured CTCs can be released with the retention of living activity, making this technique well suited for downstream applications such as drug susceptibility tests involving viable CTCs.

INTRODUCTION

Circulating tumor cells (CTCs), trace viable tumor cells that are released into the bloodstream from primary or metastatic tumor lesions, can travel through the circulatory system and form new metastatic lesions within the body.[1] CTCs have been identified as the primary cause of tumor metastasis and are even responsible for the majority of cancer-associated mortality.[2] In addition to the strong correlation with metastasis, CTCs share associated genetic and molecular information with primary and metastatic tumors. Consequently, detection of CTCs is of clinical significance in early metastasis diagnosis, progress monitoring, treatment evaluation, and the development of new therapies.[3]

The selective enrichment of CTCs from peripheral blood, which is the most critical aspect of the detection process, has been extensively studied, and various enrichment mechanisms have been proposed. At present, CTC detection techniques can be categorized into three classifications based on the specific targets or mechanisms involved.

(1) CTC isolation based on physiological characteristics. Relying on the specific physiological properties of CTCs, techniques including filtration,[4,5] centrifugation,[6,7] and microfluidics[8,9] have been developed to directly separate CTCs from blood samples. Isolation can enrich CTCs with a complete cellular structure, and high viability can be attained with elaborate manipulation. However, the physiological features of CTCs partially overlap with those of normal blood cells, leading to significant interference, particularly when considering the substantial quantitative disparity between normal blood cells and CTCs (millions of normal blood cells vs. several to dozens of CTCs per milliliter of blood, excluding red blood cells).

(2) CTC capture using surface antigens. There are various tumor-associated antigens and tumor-specific antigens (epithelial cell adhesion molecule [EpCAM], folic acid receptor, etc.) on the surface of CTCs that can be utilized as targets for their capture. The capture process commonly involves affinity binding between the surface antigens of CTCs and corresponding ligand molecules (antibodies,[10,11] aptamers,[12] etc.) decorated on well-designed materials or devices, ultimately enabling accurate counting. However, CTC capture strategies based on specific antigen recognition are inevitably accompanied by misdetection of antigen-negative CTC subpopulations. For instance, transference of CTCs usually involves epithelial-mesenchymal transition (EMT) to downregulate EpCAM expression on CTCs, while, in some cases, CTCs may lose all of their surface EpCAM molecules after undergoing EMT.[13] Consequently, the EpCAM-targeted strategies cannot be applied to the capture of EpCAM− CTCs.

(3) CTC detection by combined strategies. CTC detection based on a single strategy is usually plagued by false-negative or false-positive interference. In this regard, dual and even triple strategies combining physical screening and antigen recognition have been proposed to obtain CTCs with higher purity.[14,15] However, combined detection is complex in operation, and these time-consuming and multistep processes always lead to compromise of the viability of captured CTCs, and the accuracy of detection is also affected. As a result, despite advancement in the field of CTC detection, with several products and devices now commercially available, the absence of a universally accepted gold standard continues to hinder widespread clinical adoption.[16] Hence, further enhancing the reliability and precision of CTC detection is imperative to fully realize the potential of this technology.

It is well known that fluctuation of the CTC phenotypes, attributable to tumor heterogeneity, is the primary hindrance to the effective detection of CTCs, as different phenotypes of CTCs with dozens of subsets/subpopulations can coexist in a cancer patient.[17–19] Therefore, broad coverage of different phenotypes of CTCs is crucial to overcome this challenge. Malignant carcinomas generally undergo an extra-fast growth stage[20] because of the high intracellular metabolic activity shared by most carcinoma cells regardless of the cancer type or subpopulations, including highly active CTCs in the bloodstream.[21] In this respect, the pronounced metabolic activity difference can be exploited to discern CTCs from normal blood cells, and a precise CTCs enrichment approach can be conceived by bio-orthogonal metabolic glyco-engineering (MGE). The bio-orthogonal MGE technique is a versatile tool with simple operation.[22,23] MGE involves introducing chemical groups (azido, bicyclo[6.1.0]non-4-yn-9-yl groups, and so on) onto cell membranes by the intrinsic glyco-biosynthesis pathways in a manner that does not compromise the integrity and activity of cells. The process is usually combined with classic bio-orthogonal click reactions to anchor functional groups, motifs, or materials with the labeled cells for further investigation

and biomedical applications,[24–26] such as tumor imaging and tumor targeting. It has been demonstrated that these specific "artificial targets" can be introduced to the surface of almost all types of tumor cells.[27–29] Therefore, it may be possible to incorporate bio-orthogonal chemical motifs onto CTCs via MGE to facilitate precise recognition, efficient capture, and subsequent release of CTCs.

Here, a CTC isolation system based on the "label-capture-release" process is described for precise and efficient CTC enrichment from blood samples, followed by downstream applications using the isolated CTCs. The artificial monosaccharide tetra-acetylated *N*-azidoacetyl-D-mannosamine (Ac_4ManNAz) is used to treat the blood samples, within which only the rarely existing CTCs can be labeled with azido groups due to their abnormal glycometabolism. A capture-release dual-mode plate is prepared by introducing sequential disulfide and dibenzocyclooctane (DBCO) motifs onto the surface. This functionalized plate not only enables the capture of azido-labeled cancer cells via a copper-free click reaction[30] between the DBCO and azido groups but also allows non-destructive release of the captured cells in the ensuing disulfide reduction.[31] This system has the potential for broad-spectrum, direct, and accurate CTC recognition of various phenotypes despite interference from normal blood cells. The results demonstrate that multiple types of tumor cells with the EpCAM+ and EpCAM−phenotypes, in both adherent and suspended states, are labeled effectively. All of the epithelial, interstitial, and hybrid phenotypes of CTCs can be separated from clinical blood samples of cancer patients. Furthermore, this robust system ensures the preservation of cell activity following release and exhibits ultralow nonspecific adsorption of white blood cells (WBCs) under the same conditions. These advantages make it highly valuable in non-invasive cancer diagnosis and facilitate downstream applications of CTCs, such as drug susceptibility evaluation, as demonstrated in this study.

MATERIALS AND METHODS

Materials

DBCO-*N*-hydroxysuccinimide (NHS), DBCO-NH_2, DBCO-biotin, and MAM-biotin were bought from Ruixi (China). All fluorescently labeled protein probes were supplied by Univbio (China). All clinically used gene probes (Fisher standard) and membranes with a diameter of 8 μm (isolation by size of epithelial tumor cells [ISET] standard) were bought from Xingyuan (China). Doxorubicin (DOX), cisplatin (CDDP), and paclitaxel (PTX) were provided by Shenzhen People's Hospital.

CTCs captured by the bio-orthogonal films and identified by nucleus/CD45/EpCAM/vimentin staining

EDTA anticoagulant-treated whole-blood samples were obtained from different cancer patients at Shenzhen People's Hospital as well as healthy people. Each blood sample was pretreated with the ammonium-chloride-potassium (ACK) lysis buffer at 0°C for 10 min and collected by centrifugation at 300 × *g*. After washing with PBS containing 2% fetal bovine serum (FBS), the remaining cells were cultured in the serum-free lymphocyte culture medium containing 100 μM Ac_4ManNAz for 12 h. The treated cells were washed with PBS 3 times, added to chitosan film (CF)-nanoparticale (NP)-DBCO on a 24-well plate, and shaken at 20 rpm for 1 h. The samples were rinsed with PBS at least 5 times, and the cells were fixed by 4% paraformaldehyde and Triton X-100 (0.1% in H_2O, 5 min). Finally, the fixed cells were treated with the Cy3-labeled EpCAM gene probe (50 μM, 1 h), Alexa Fluor 488-labeled vimentin gene probe (50 μM, 1 h), Alexa Fluor 750-labeled CD45 gene probe (100 μM, 3 h), and DAPI (10 μg/mL, 3 min) according to manufacturer's instructions. An automatic scanning fluorescence microscope (Axio Imager Z2, Carl Zeiss, Germany) was used to identify the captured CTCs as nucleus+/CD45−/EpCAM+ and/or vimentin+.

CTCs released from the bio-orthogonal films and examined for viability

EDTA anticoagulant-treated whole-blood samples were obtained from different cancer patients at Shenzhen People's Hospital. Each blood sample was processed by our capture workflow using CF-NP-disulfide (SS)-DBCO films as described above. Afterward, DTT (10 mM) in the culture medium was added for 40 min to allow the release of captured CTCs. The released cells were collected and cultured with medium containing the Alexa Fluor 647-labeled CD45 probe (50 μM, 15 min) and Hoechst-33342 (10 μM, 15 min) to identify CTCs as nucleus+/CD45−, with viability examined by Calcein-AM/propidium iodide staining (100 μM, 30 min). Finally, the medium (20 μL) was added to a confocal dish with a 3 × 3 mm hole and observed under a confocal microscope (STEDYCON, Leica, Germany).

Drug susceptibility tests using CTCs

EDTA anticoagulant-treated whole-blood samples (20 mL) were obtained from different cancer patients at Shenzhen People's Hospital. Each blood sample was pretreated with ACK lysis buffer at 0°C for 10 min and collected by centrifugation at 300 × *g*. After washing with PBS containing 2% FBS, the remaining cells were evenly divided into 4 portions and then cultured in serum-free lymphocyte culture medium containing Ac_4ManNAz (100 μM) and different drugs at 35% maximal inhibitory concentration (IC_{35}) for 24 h. Subsequently, the treated cells were processed by our capture-release workflow using CF-NP-SS-DBCO films as described above. The released cells were incubated with DBCO-biotin (100 μM, 1 h) and MAM-biotin (200 μM, 1 h) in the labeling buffer for 1 h at room temperature, washed 3 times with the labeling buffer (each time at least 10 min), and then incubated with a mixture of Hoechst-33342 (10 μM, 15 min)/Alexa Fluor 488-labeled streptavidin (50 μM, 15 min)/Alexa Fluor 647-labeled CD45 (50 μM, 15 min)/Alexa Fluor 594-labeled EpCAM-cytokeratins (CKs) (50 μM, 15 min) in the dark. After fluorescent staining, the medium (20 μL) was added to a confocal dish with a 3 × 3 mm hole and observed under a confocal microscope (STEDYCON, Leica). The CTCs were identified as nucleus+/CD45−/EpCAM−CKs+. The total fluorescence intensity (FI) of Alexa Fluor 488 and area (S) was examined on all detected CTCs using ImageJ software, and the relative FI (RFI) was calculated using the formula $RFI = FI / \{2\pi [(S / \pi)^{0.5}]\}$. The drug sensitivity was characterized by the ratio of RFI between the experimental group and the control group.

Ethics statement and patient consent

This clinical study was approved by the Ethics Committee of Shenzhen People's Hospital, China (approval number KY-LL-2020157-02). All participants provided written informed consent for sample collection and subsequent analysis.

RESULTS

Optimization of the MGE condition

The conjugation of artificial groups onto viable cells has been achieved by several intrinsic biosynthetic pathways, including the classic Roseman-Warren route,[32] galactosamine salvage route,[33] and fucose salvage route.[34] Notably, both tumor cells and normal cells can be labeled by MGE; however, there are differences between normal blood cells and CTCs in the blood of cancer patients. Therefore, selective labeling of CTCs from normal blood cells is critical to the isolation strategy. The ideal outcome is that tumor cells are discerned from peripheral blood mononuclear cells (PBMCs; chosen as the representatives of WBCs) by the process of MGE.

To optimize the MGE condition, MCF-7 cells and H524 cells with different biochemical characteristics (with EpCAM+ and EpCAM− phenotypes, in adherent and suspended states, respectively) are employed to mimic the heterogeneous CTCs. The monosaccharide Ac_4ManNAz with azido groups is utilized due to its involvement in intracellular glyco-biosynthesis following co-incubation, introducing the azido groups via the Roseman-Warren biosynthetic pathway (Figure 1A). The azido groups on the cells can react with the DBCO-biotin molecules in the copper-free click reaction, resulting in the immobilization of biotin motifs, and the treated cells can be subsequently labeled with green fluorescence via specific binding between biotin and streptavidin-Alexa Fluor 488 (streptavidin-AF488).[35] Therefore, the FI of cells after staining is positively related to the abundance of azido groups, which depends on the amount of added Ac_4ManNAz and the duration of co-incubation.

In the process, the cells are first incubated with different concentrations of Ac_4ManNAz for 24 h to determine the maximum allowable concentration. As shown in Figure 1B, no obvious cytotoxicity is observed when MCF-7 cells, H524 cells, and PBMCs are cultured with Ac_4ManNAz at a concentration below 125 μM. It is evident that both types of tumor cells are labeled by Ac_4ManNAz in a concentration-dependent manner, and the FI from the labeled MCF-7 and H524 cells changes only slightly when the concentration of added Ac_4ManNAz is increased from 75 μM to 100 μM (Figures 1C and S1), indicating that the azido groups are almost saturated at these concentrations. In contrast, the green fluorescence detected from PBMCs is weak despite an Ac_4ManNAz concentration of 100 μM. Accordingly, the optimal concentration of Ac_4ManNAz is determined to be 100 μM.

Since the metabolic activity of CTCs and normal blood cells diminishes with time after extraction from blood vessels,[36] the duration of the MGE condition is optimized. Here, the different cells are incubated with 100 μM of Ac_4ManNAz for 4, 8, 12, and 24 h prior to fluorescent staining. As demonstrated in Figures 1D and S2, both the MCF-7 cells and H524 cells exhibit maximum FI after culturing for 12 h, with the relative FI of MCF-7 cells even higher than that of H524 cells, whereas fluorescence from the stained PBMCs is negligible under the same conditions. The FI of the labeled cancer cells is at least 40 times higher than that of

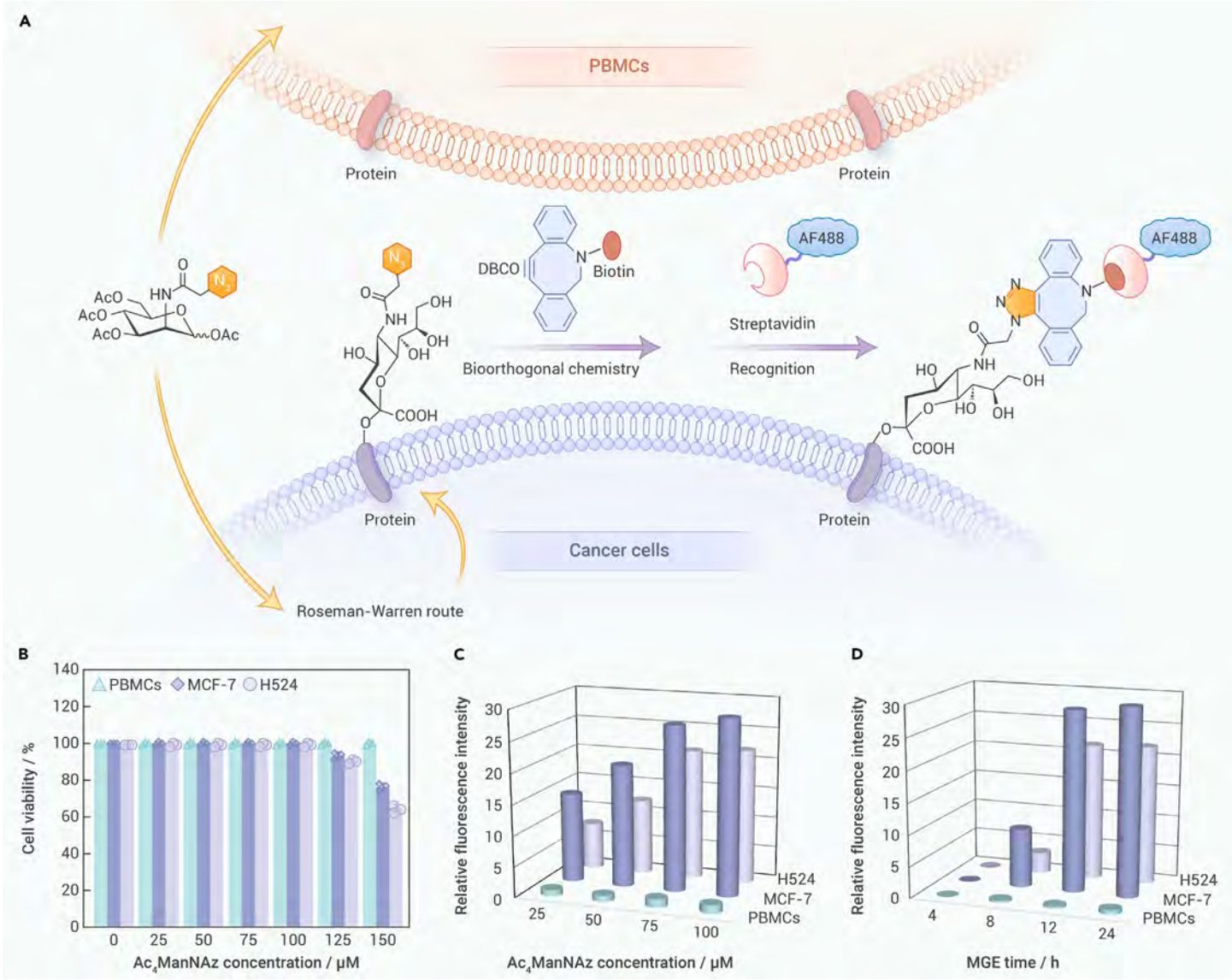

Figure 1. MGE process and fluorescent labeling (A) Schematic showing the introduction of azido groups onto cells via the Roseman-Warren route and selective labeling of cells by DBCO-biotin/streptavidin-AF488. (B) Monosaccharide concentration-cell survival rate diagram for the determination of the maximum allowable concentration of $Ac_4ManNAz$. (C) Monosaccharide concentration-cell surface FI diagram explaining the influence of the $Ac_4ManNAz$ concentration on labeling efficiency. (D) MGE time-cell surface FI diagram explaining the influence of the MGE time on labeling efficiency.

the labeled PBMCs, indicating that tumor cells are specifically labeled with the MGE technique. Additional results reveal that five other types of tumor cells (A549, Jurkat, HeLa, Huh-7, and HepG2 cells) can be labeled under the same conditions (Figure S3). Consequently, a phenotype-independent MGE labeling technique (100 μM $Ac_4ManNAz$ and co-culturing for 12 h) is employed in the subsequent CTC isolation study.

Design, preparation, and characterization of bio-orthogonal films

The capture of CTCs using bulk biomaterials has been explored, and nanostructures with a large surface area are usually prepared on planar biomaterials to enhance the interactions between CTCs and functionalized surfaces.[37–39] Anti-fouling is another requirement for the CTC-capturing surface, and it is essential to reduce and even avoid nonspecific adsorption of normal blood cells during the capture process. Moreover, the functional motifs on the CTC-capturing surface can be engineered with breakable bonds to facilitate the release of captured CTCs. Based on all of these considerations, surface coatings are designed for the subsequent capture and release study of the azido-labeled CTCs.

Three DBCO-functionalized chitosan coatings (CF-DBCO, CF-NP-DBCO, and CF-NP-SS-DBCO) are deposited on glass plates for the capture/release study (Figure 2A). Chitosan, a polysaccharide prepared by partial de-acetylation of the -NHAc group on chitin, is chosen as the base material because of good biocompatibility and provision of multiple free amino groups as reaction sites for conjugation.[40,41] CF-DBCO denotes the chitosan film directly immobilized with the DBCO functional groups, whereas CF-NP-DBCO involves the introduction of DBCO-functionalized nanoparticles onto the chitosan film to enhance the anti-fouling effect.[42] The CF-NP-SS-DBCO coating has additional di-sulfide groups compared to CF-NP-DBCO so that it can be readily reduced to release the captured cells in a mild and non-destructive way.

For the fabrication of CF-DBCO, the chitosan film is deposited on a glass plate by spin coating, followed by treatment with NaOH to expose the amino groups. The chitosan film reacts with DBCO-NHS ester in ethanol to yield CF-DBCO. For fabrication of the CF-NP-DBCO and CF-NP-SS-DBCO films, sulfobetaine methacrylate, methacrylic acid, and *N,N′*-methylenebisacrylamide are adopted for polymerization during refluxing to produce zwitterionic sulfobetaine-type nanoparticles with a diameter of about 100 nm (Figure 2B).[43] The nanoparticles have abundant carboxylic acid groups, which can be immobilized on the chitosan films by the amidation reaction. There are partial carboxylic acid groups on the nanoparticles on the side opposite the substrate, and the CF-NP-DBCO and CF-NP-SS-DBCO films are fabricated by subsequent amidation of the remaining carboxylic acid groups with DBCO-NH_2 and DBCO-SS-NH_2 groups, respectively (Figure S5).

The three functionalized samples are characterized by scanning electron microscopy (SEM), energy-dispersive X-ray spectroscopy (EDS), and X-ray

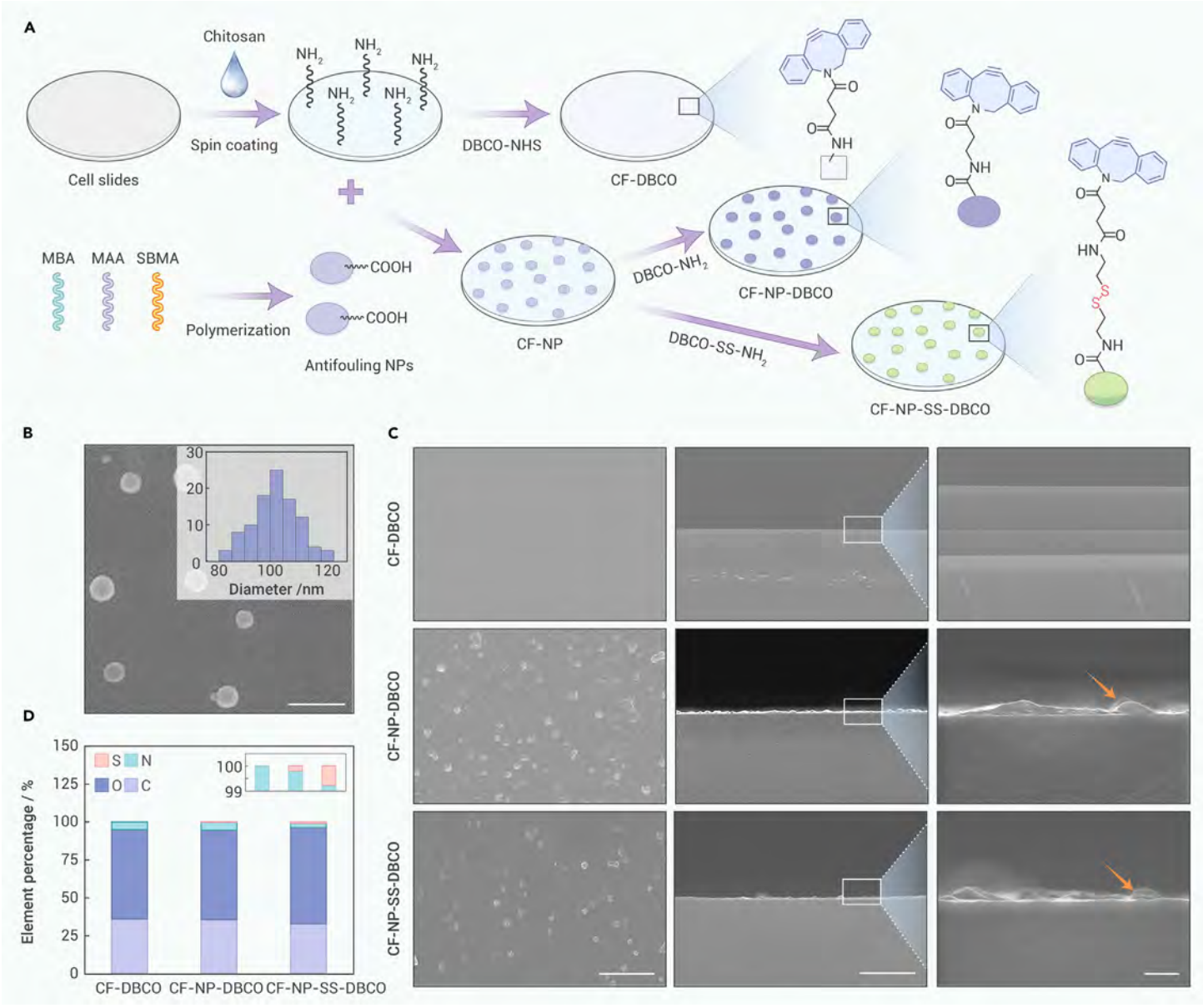

Figure 2. Design, synthesis, and characterization of bio-orthogonal films (A) Schematic showing the preparation of different bio-orthogonal films (refer to Figure S4 for the synthesis details). (B) SEM image and size distribution of the anti-fouling nanoparticles (scale bar: 200 nm). (C) SEM images of the front and section of different bio-orthogonal films (red arrows indicate embedded nanoparticles) (scale bars: 5 μm, 5 μm, and 500 nm from left to right). (D) EDS elemental analysis of different bio-orthogonal films.

photoelectron spectroscopy (XPS). As shown in Figure 2C, the CF-DBCO film consists of three distinct layers (a DBCO-containing layer, alkalized layer, and acetate layer, from top to bottom) with an overall thickness of around 3 μm. The SEM images of CF-NP-DBCO and CF-NP-SS-DBCO substrates reveal that the anti-fouling nanoparticles are dispersed on the films and spread like fried eggs with a diameter of about 400 nm. EDS and XPS results (Figures 2D and S6) verify that DBCO motifs exist on all the three films and confirm the presence of sulfur on CF-NP-SS-DBCO.

Selective capture and release of cancer cells

After determining the MGE conditions and preparation conditions of different DBCO-functionalized films, the capture and release of CTCs is assessed (Figure 3A). As MGE is phenotype independent, H524 cells that resemble the suspension status of CTCs in circulation are chosen based on the optimized MGE conditions (culturing with 100 μM Ac_4ManNAz for 12 h). It is assumed that the labeled cells can be captured by the functionalized films via a strain-promoted azide-alkyne cycloaddition (SPAAC) reaction between the azido groups on the tumor cells and DBCO groups immobilized on the films. In the comparative study of the azido-positive and azido-negative cells, the H524 cells are treated with Ac_4ManNAz (an azido-positive monosaccharide) and Ac_4ManNAc (an azido-negative monosaccharide), respectively, because both of them can be taken up and metabolized by cancer cells. After MGE labeling, the treated cells are incubated with the three DBCO-functionalized films to allow CTC capture in a spontaneous and time-dependent manner. As shown in Figures 3B and S7, approximately 80% of the azido-labeled H524 cells (~40,000 of 50,000 cells) are captured by the DBCO-functionalized films within 1 h, and prolonging the capture time causes negligible improvement for the three films. This is due to the surface saturation, and the capacity is more than sufficient for CTC detection, as the amounts of CTCs in typical clinical samples are quite low (several to dozens of CTCs per milliliter of blood). Although the CTC capture capability of different samples is similar, the anti-fouling effects of the CF-DBCO film are inferior to those of the nanoparticle-decorated ones. A small proportion of the azido-negative H524 cells is absorbed onto the CF-DBCO film, whereas almost no nonspecific absorption is observed on the CF-NP-DBCO and CF-NP-SS-DBCO films (Figures 3B and S7).

To further corroborate the biological properties, tests are carried out with both PBMCs and H524 cells. The H524 cells (~50,000 cells) and PBMCs from 1 mL of healthy blood (~4–8 million cells) are initially subjected to standard MGE labeling. Under these conditions, the CF-DBCO film exhibits severe nonspecific adsorption of PBMCs without azido groups, while only trace amount of PBMCs

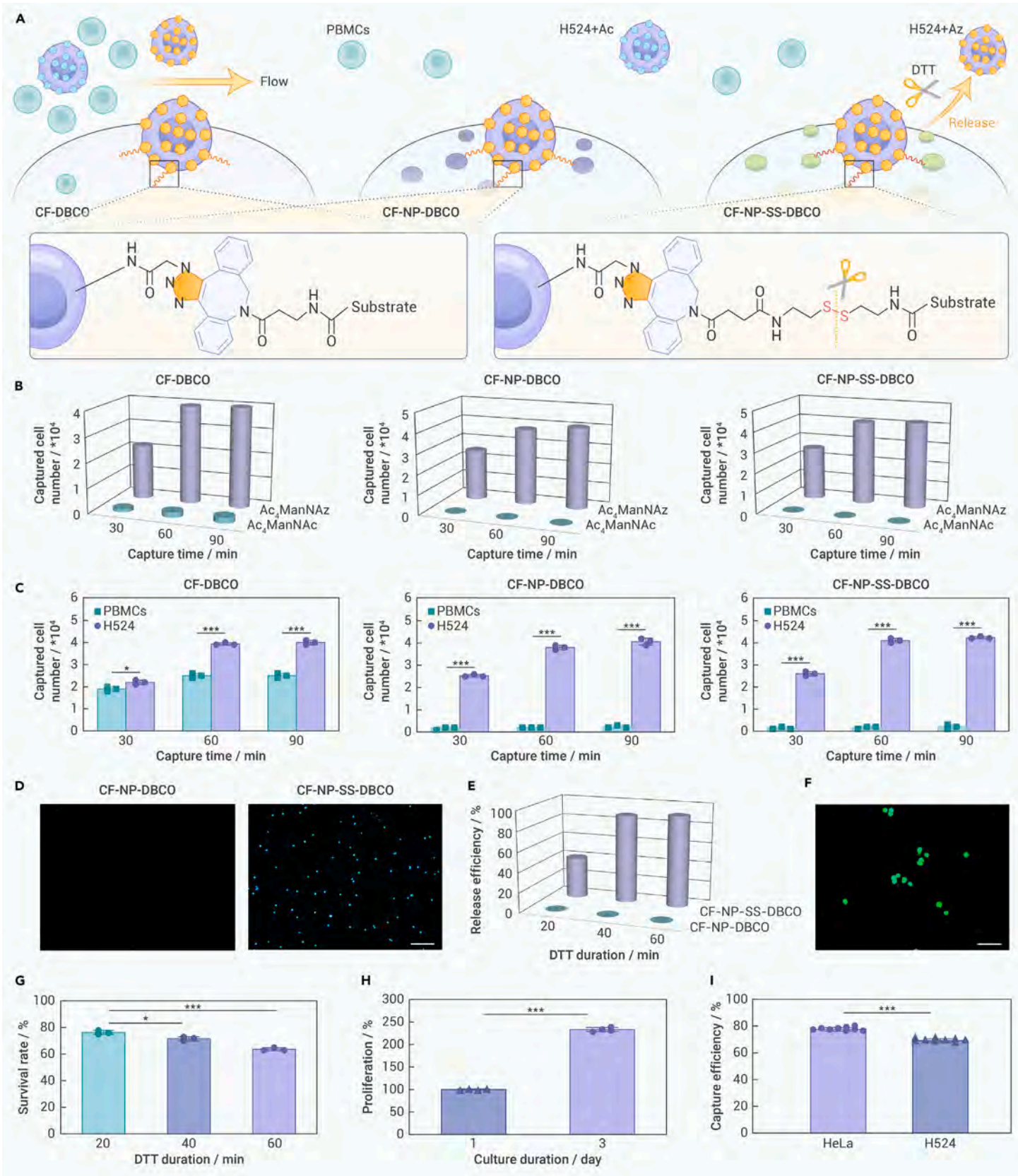

Figure 3. Selective capture and release of cancer cells by bio-orthogonal films (A) Schematic of the capture-release process of cancer cells. (B) The relationship between capture time and the number of captured cells (from a total of 50,000 cells) of MGE-treated H524 cells with or without azido groups. (C) The number of captured cells over time (from ~50,000 H524 cells or PBMCs from 1 mL of healthy blood [~4–8 million cells]) of MGE-treated H524 cells and PBMCs. (D) Fluorescence microscopy images of H524 cells (stained with DAPI) after release (scale bar: 100 μm). (E) Correlation between DTT treatment duration and cell release efficiency for CF-NP-DBCO and CF-NP-SS-DBCO. (F) Live/dead staining image (green for live, red for dead) of H524 cells released from CF-NP-SS-DBCO after 40 min of DTT treatment (scale bar: 50 μm). (G) Survival rates of H524 cells as a function of DTT treatment duration for CF-NP-SS-DBCO. (H) Long-term viability of H524 cells after capture and release. (I) Artificial CTC capture efficiency of CF-NP-DBCO.

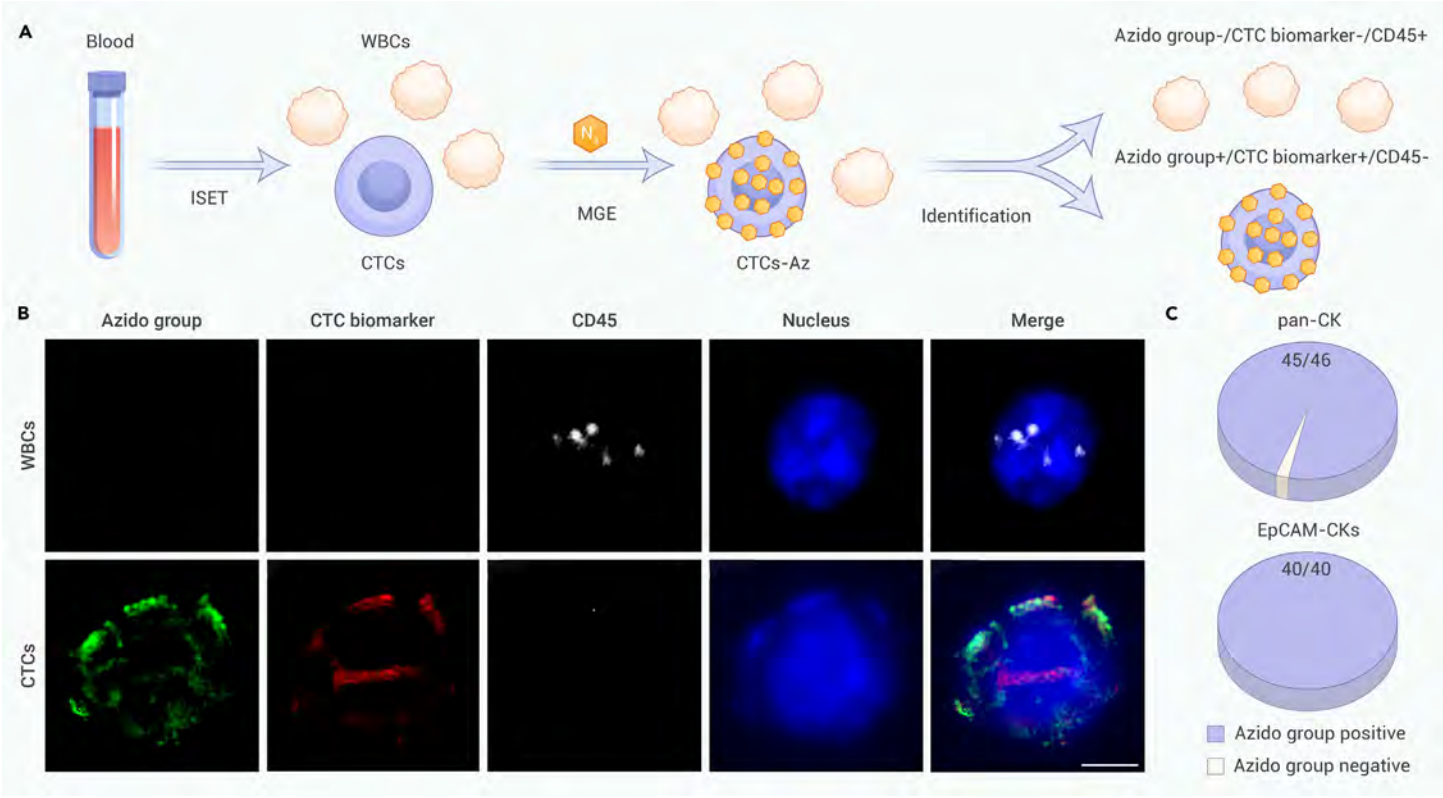

Figure 4. Selective labeling of CTCs in clinical samples by MGE (A) Flow chart of clinical CTC isolation by ISET, MGE treatment process, and immunofluorescence analysis with a combination of nucleus/CD45/CTC marker/azido fluorescent staining (pan-CK represents a mixture of CK1, CK3-8, CK10, and CK13–CK19; EpCAM-CKs represents a mixture of EpCAM, CK8, CK18, and CK19). (B) Identification of WBCs and CTCs through immunofluorescence analysis (scale bar: 5 μm). (C) Statistical analysis of the azido-labeled CTCs in blood samples.

are observed from the CF-NP-DBCO and CF-NP-SS-DBCO films (Figure 3C), thus confirming the excellent anti-fouling effects. Furthermore, this strategy is successful in capturing cancer cells of multiple sizes (Figure S8). Compared to CF-NP-DBCO, CF-NP-SS-DBCO has additional disulfide groups, and the release ability is studied using DTT to reduce the disulfide bonds. As shown in Figures 3D, 3E, and S9, only the CTCs captured by CF-NP-SS-DBCO are released upon addition of DTT. The release of CTCs is also time dependent, with more than 90% of the captured cells being released in 40 min. Most of the released cells remain alive after 40 min of DTT treatment (Figures 3F and 3G), and their long-term viability is even comparable to that of normal cells (Figures 3H and S10). Considering both the capture efficiency and anti-fouling effects, the CF-NP-DBCO and CF-NP-SS-DBCO films are significantly more favorable than the CF-DBCO substrate.

Artificial CTC detection using spike-in blood samples

To verify the feasibility and reliability of our system, a straightforward simulated experiment is designed for the detection of artificial CTCs. The artificial CTCs are prepared by spiking HeLa cells or H524 cells (~100 cells) into 1 mL of fresh blood samples (containing ~4–8 million WBCs) collected from healthy donors, and then the mixtures are pre-treated with ACK lysis buffer to remove red blood cells. The remaining cells are collected and subjected to a standard MGE labeling process in the serum-free lymphocyte culture medium. After labeling, the mixed samples are incubated on the CF-NP-DBCO film to allow the capture of artificial CTCs. The captured cells are examined by immunofluorescent staining using nucleus/CD45/pan-CK dyes, and most of them share the feature of tumor cells as nucleus+/CD45−/pan-CK+ (Figure S11). The artificial CTCs can be selectively labeled by MGE and subsequently captured by the bio-orthogonal films, even in the presence of millions of WBCs. According to the statistical results, nearly 80% of the HeLa cells and 70% of the H524 cells introduced to the blood samples can be captured by this strategy (Figure 3I). It is especially encouraging that the background WBCs show little interference in the labeling and capture process.

Selective labeling of CTCs by MGE

As mentioned above, metabolic labeling trace CTCs with phenotypes different from millions of normal WBCs is required for clinical application. Therefore, the feasibility of MGE labeling is evaluated after isolation of CTCs from four samples with three different cancer types using commercial ISET products (Figure 4A). Here, the whole-blood sample (5 mL) collected from each cancer patient is pre-treated with the ACK lysis buffer to remove red blood cells and then filtered with membranes with standard 8-μm-diameter holes to obtain CTCs. CTCs and some WBC contaminants are collected and processed under the standard MGE conditions in the serum-free lymphocyte culture medium. Identification of CTCs is performed by immunofluorescence analysis with nucleus/CD45/pan-CK/azido or nucleus/CD45/EpCAM-CKs/azido fluorescent staining. CTCs are identified as nucleus+/CD45− together with at least one clinical CTC biomarker positive (pan-CK or EpCAM-CKs) and WBCs as nucleus+/CD45+ with clinical CTCs biomarker being negative.

As illustrated in Figure 4B, the CTCs that are nucleus+/CD45−/pan-CK+ or nucleus+/CD45−/EpCAM-CKs+ can be labeled by our MGE strategy (green fluorescence). Among the 46 CTCs identified by the pan-CK marker, 45 are successfully labeled with azido groups, and all 40 CTCs identified by the EpCAM-CKs marker are labeled with azido groups (Figures 4C, S12, and S13). The results demonstrate the feasibility of selective labeling of CTCs in clinical samples by MGE and suggest that the artificial groups introduced to the CTCs via MGE can be used as general neo-markers for CTC detection.

Phenotype-independent capture and release of CTCs by bio-orthogonal films

To investigate the clinical applicability of the detection system, 1 mL of whole blood collected from 8 randomly selected cancer patients (P1–P8) and 2 healthy people (H1 and H2) (for detailed information about donors, please see Table S1) is pre-treated with the ACK lysis buffer to remove red blood cells and then subjected to standard MGE labeling in the serum-free lymphocyte culture medium. The treated cell mixtures are then incubated on the bio-orthogonal films to allow CTCs to be captured via the SPAAC reaction. Since the results of azido group labeling correlate with those of pan-CK/EpCAM-CKs staining of CTCs, cross-validation is performed to classify the subsets of captured CTCs. The cells on the bio-orthogonal surface are analyzed by immunofluorescent analysis with nucleus/CD45/EpCAM/vimentin staining, in which three general CTC subsets can be

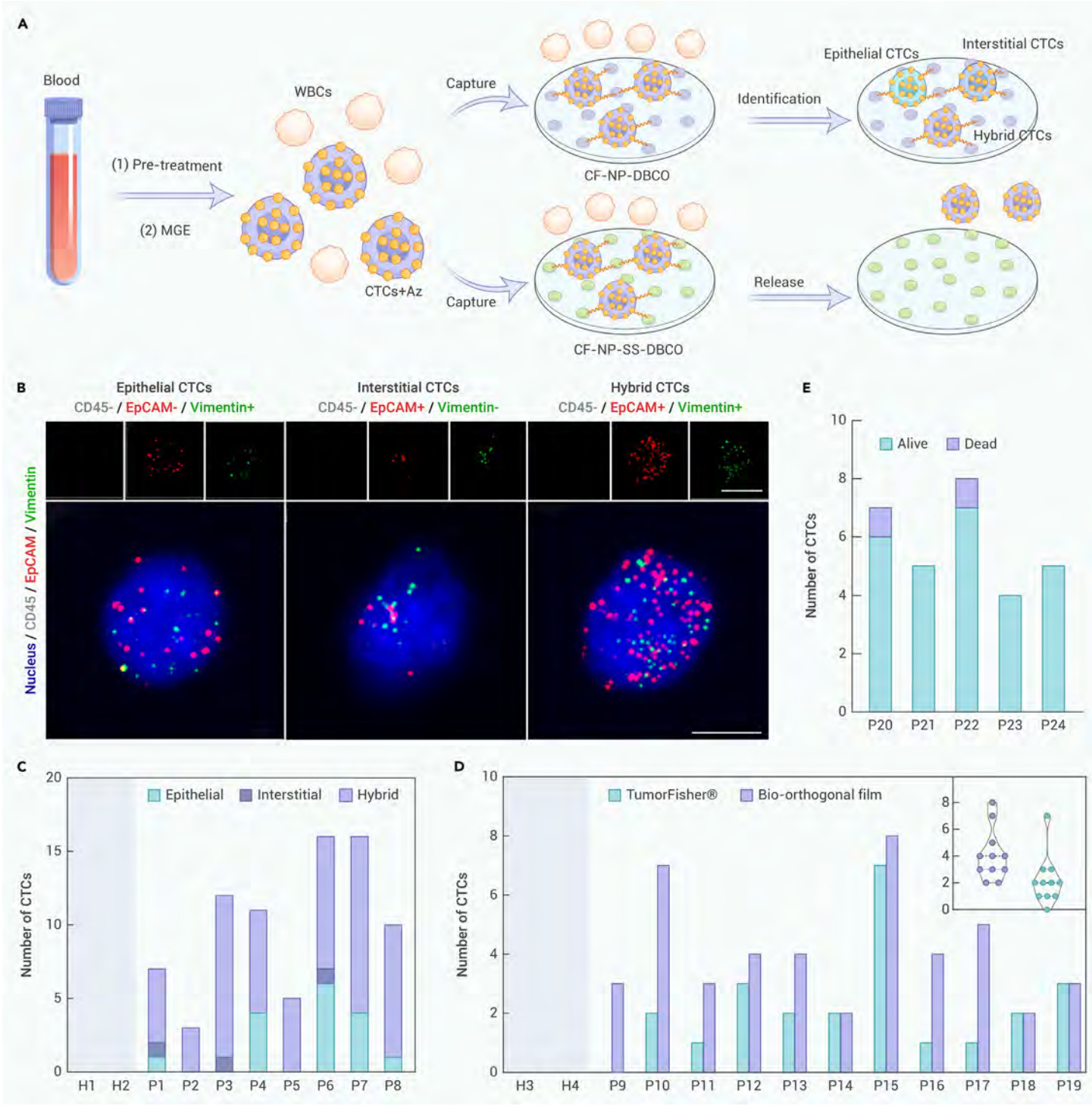

Figure 5. Capture and release of CTCs from blood samples by bio-orthogonal films (A) Schematic of the capture-release process of CTCs. (B) General view of different phenotypes of captured CTCs identified by immunohistochemical staining (scale bars: 10 μm for small pictures and 5 μm for large pictures). (C) Statistical chart of the captured CTCs with different phenotypes. (D) Direct comparison of CTC detection between our strategy and the TumorFisher system. (E) Statistical chart of the released CTCs examined by live/dead staining.

classified as epithelial CTCs (nucleus+/CD45−/EpCAM+/vimentin−), interstitial CTCs (nucleus+/CD45−/EpCAM−/vimentin+), and hybrid CTCs (nucleus+/CD45−/EpCAM+/vimentin+). For EpCAM and vimentin staining, fluorescence of ≤7 is considered a negative result.[44] As shown in Figure 5B, all epithelial, interstitial, and hybrid CTCs can be captured by the bio-orthogonal system. The introduction of neo-markers (azido groups) enables precise detection of heterogeneous CTCs in the clinical samples. Based on the immunofluorescence staining results displayed in Figure S14, the CTCs in different blood samples were counted and are shown in Figure 5C. It is clear that all blood samples from different cancer patients (P1−P8) tested positive for CTCs, while those from healthy people (H1 and H2) showed negative CTCs results. Another advantage of the detection system lies in its low nonspecific adsorption of WBCs on the films due to the anti-fouling effects. Compared to the previously reported methods for CTC detection, the level of background interference from WBCs remains minimal when using the bio-orthogonal films (Table S2).

Encouraged by these results, a direct comparison is carried out between our method and the clinically approved CTC detection system called TumorFisher, which captures CTCs via EpCAM recognition. Blood samples are collected from 11 additional patients with different cancers (P9−P19) and 2 healthy donors (H3 and H4). Each blood sample is halved and processed in parallel by

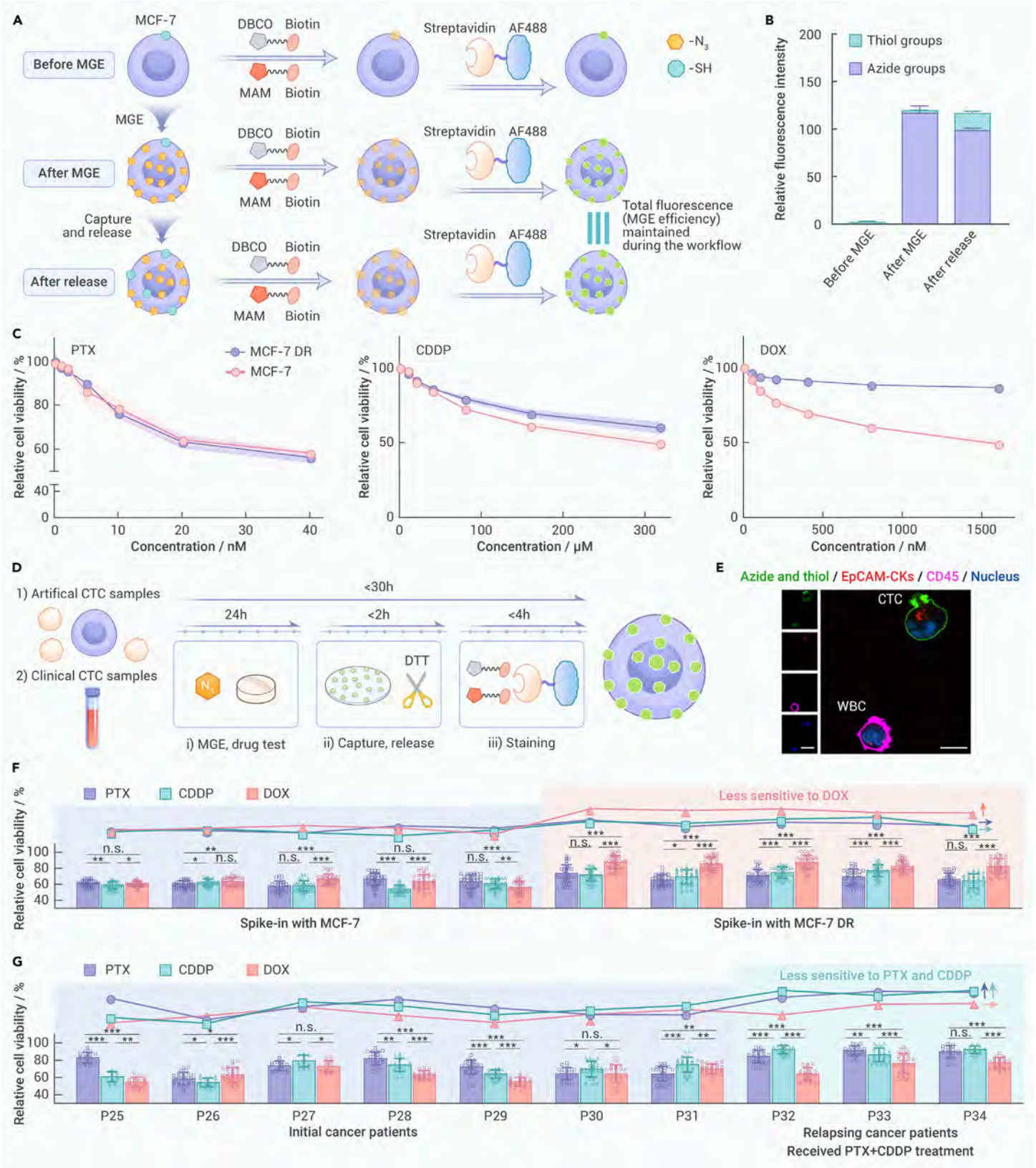

Figure 6. Real-time drug susceptibility assessment based on the MGE efficiency of released CTCs (A) Schematic illustrating fluorescence labeling of the azide and thiol groups on cancer cells. (B) Quantitative fluorescence analysis of the azide and thiol groups on cancer cells. (C) Drug concentration-relative cell viability of MCF-7 cells and MCF-7 DR cells determined by MGE fluorescence labeling. (D) Flow chart illustrating the workflow of real-time drug susceptibility tests. (E) General view of WBCs and CTCs identified by immunohistochemical staining (scale bars: 20 μm for small pictures and 10 μm for the large picture). (F) Statistical chart of real-time drug susceptibility tests using spike-in samples. (G) Statistical chart of real-time drug susceptibility tests using clinical samples.

TumorFisher and our detection workflow, and the captured CTCs are then identified by immunofluorescent staining. As shown in Figures 5D and S15, in addition to the negative detection results of healthy donors (H3 and H4), our strategy is successful in the trace detection of CTCs from all 11 cancer patient blood samples. In contrast, 10 of 11 cancer patient blood samples show positive results, but P9 with colon cancer (partly mesenchymal tissue tumor) is

misdetected (giving a false-negative result) by the commercial TumorFisher system. Our strategy is demonstrated to not only outperform the TumorFisher system for the clinical CTC detection of mesenchymal tissue tumors (P9, 3 vs. 0; P10, 7 vs. 2; P11, 3 vs. 1) but also has superior detection capability for other cancer types (P12–P19, 5 wins and 3 draws) (Figure S15). The label-capture-release process is carried out on 5 other cancer blood samples (P20–P24), and the results are in line with expectations, revealing that most of the CTCs can be captured and released from the CF-NP-SS-DBCO film while maintaining their living activity (Figure 5E).

Real-time drug susceptibility assessment using viable CTCs

As mentioned previously, high intracellular metabolic activity is shared by most cancer cells, including CTCs. This fact suggests that the MGE efficiency of viable CTCs may be correlated with the pathological features of cancer patients, which bodes well for the *in vitro* assessment of drug susceptibility. Conventional drug susceptibility tests still require the pre-culture of isolated CTCs for weeks to months,[45,46] significantly delaying therapeutic decisions. To address this limitation, we establish a real-time methodology by directly evaluating the MGE efficiency of CTCs after different drug treatments, eliminating the need for time-consuming cell culturing to achieve faster and more efficient cancer therapy.

Prior to the involvement of rare CTCs, we first evaluate the influence of the workflow on the MGE efficiency of cancer cells. The typical breast cancer cells (MCF-7 cells) are subjected to MGE labeling, and then the azide and thiol groups on the cell surface are quantified together. This is necessary because a small proportion of the azide groups is converted 1-1 to thiol groups during the capture-release process. As shown in Figure 6A, the azide and thiol groups on the cell surface are converted to biotin markers by DBCO/azide and maleimide/thiol reactions, and subsequently, green fluorescence can be achieved by specific biotin/streptavidin-AF488 binding. Quantitative fluorescence analysis reveals that the total amount of thiol and azide groups on the cell surface are almost unaffected by the capture-release process. Furthermore, the functional groups naturally present on the cell surface are negligible (<3%) compared to those introduced by MGE (Figure 6B).

The feasibility of MGE fluorescence labeling in the drug sensitivity test is investigated using three antineoplastic drugs, DOX, CDDP, and paclitaxel (PTX),[47] which are used to treat MCF-7 cells and those resistant to DOX (MCF-7 DR cells). Then, 40 randomly selected cells in each group are analyzed, and the average FI is determined by dividing the total FI by the cell circumference. For reference, cells after different treatments are also examined by the CCK-8 assay (Figure S16). Figure 6C shows that all three antitumor drugs affect the MGE efficiency of MCF-7 cells in a dose-dependent manner, which is in general agreement with the CCK-8 results. In contrast, the MCF-7 DR cells are much less sensitive to DOX, as shown by both the MGE fluorescence labeling and the CCK-8 assay. MGE fluorescence labeling not only is superior to the CCK-8 assay by requiring fewer cells (few to tens vs. tens of thousands) but also fares better in evaluating the therapeutic effect of PTX-treated groups (Figures 6C and S16). After thorough evaluation, the IC_{35} for different drugs (DOX, 624 nM; CDDP, 139 μM; PTX, 20 nM) is used in the following drug sensitivity tests involving artificial and real CTCs (Figure 6D).

To mimic clinical applications, artificial CTCs are prepared by spiking MCF-7 cells or MCF-7 DR cells (~500 cells) into 20 mL of fresh blood samples. Different drug treatments are performed, and the viability of artificial CTCs is determined by MGE fluorescence labeling. Given that MCF-7 cells are EpCAM-CKs+, CD45 and EpCAM-CKs antibodies are used to distinguish the WBCs and artificial CTCs (Figure 6E). The findings indicate that different drug treatments can impair the MGE efficiency of artificial CTCs, but their effects on MCF-7 spike-in samples are random. In sharp contrast, the artificial CTCs prepared by MCF-7 DR strain display significantly reduced sensitivity to the DOX treatment (Figure 6F).

Encouraged by the results of the spike-in experiments, drug susceptibility tests using clinical CTCs are performed. The blood samples from 7 initial breast cancer patients (P25–P31) and 3 relapsing cancer patients who had received the PTX+CDDP treatment (P32–P34) are processed in parallel. As shown in Figure 6G, the CTCs from the 7 initial cancer patients show diverse sensitivities to different drugs, whereas those from the 3 relapsing patients who had undergone PTX+CDDP therapy are most sensitive to the DOX treatment. Overall, the feasibility of our strategy for the isolation of viable CTCs and subsequent drug susceptibility evaluation has been validated.

DISCUSSION

After decades of continuous exploration, significant progress has been made in the detection of CTCs. The Cellsearch system was the first US Food and Drug Administration-approved product for CTC detection, targeting the EpCAM antigens on CTCs. Meanwhile, the ISET membrane has been developed to obtain CTCs with intact morphology by physical filtration. Several microfluidics systems have also been developed for direct enrichment of CTCs in blood samples with high throughput.[8,9] Nowadays, novel CTC detection techniques with combined mechanisms are emerging, but a deeper understanding of the high heterogeneity of CTCs requires more precise and efficient isolation, and the recognition of rare CTCs from millions of WBCs remains a critical challenge as well. In this respect, the high cellular activity of CTCs originating from abnormal intracellular metabolism provides a promising target for recognition. Metastasis begins at a very early stage of cancer, while most of the tumor cells released from lesions die of shear stress, anoikis, or immune attack. Consequently, only a small fraction of highly active tumor cells can survive and turn into CTCs. The high activity is shared by all CTCs, regardless of their phenotypes, subsets, and subpopulations.

In this study, Ac_4ManNAz, a monosaccharide utilized for MGE labeling of dozens of different tumor cells, has been demonstrated to be able to distinguish CTCs from WBCs through the optimized MGE labeling process. By adjusting the MGE conditions, artificial neo-markers (azido groups) can be selectively introduced onto CTCs without compromising their integrity. The condensed neo-markers serve as recognition tags for subsequent capture of CTCs. Although our study demonstrates the great potential of MGE for precise labeling of CTCs, it should be noted that the Ac_4ManNAz monosaccharide metabolized by the Roseman-Warren route is only one of the options, and future research can explore CTC capture using alternative MGE routes.

Another key aspect of our study is the design and functionalization of CTC capture devices. The interactions between rare CTCs and solid surfaces are prone to interference by millions of WBCs as well as abundant biomolecules in blood samples. Therefore, surface functionalization of the CTC capture device with anti-fouling capability is essential. Instead of the conventional CF-DBCO film, the nanoparticle-modified CF-NP-DBCO and CF-NP-SS-DBCO films are preferable for minimizing nonspecific absorption of WBCs. This is because the nanoparticles are composed of the zwitterionic sulfobetaine motif, which has good cytocompatibility and strong anti-fouling effects and is promising for the modification of CTC capture devices. Furthermore, the CF-NP-SS-DBCO films are designed with breakable disulfide bonds, facilitating the release of viable CTCs for various downstream applications. As a proof of concept, we succeed in obtaining viable CTCs from cancer blood samples and directly performing real-time drug susceptibility tests without long pre-culturing. We are currently conducting clinical trials, especially follow-up studies, and will present our new results in due course.

CONCLUSION

A novel CTCs isolation strategy based on the glycometabolic difference between CTCs and normal blood cells is designed and demonstrated. By pre-treating clinical blood samples together with MGE labeling, multifunctional bio-orthogonal films enable the capture of CTCs in a phenotype-independent manner. Our strategy is superior to the commercialized TumorFisher system in terms of broad-spectrum and accurate CTC detection. Furthermore, most of the captured CTCs can be released from the bio-orthogonal films with maintained viability, allowing real-time drug susceptibility assessment using viable CTCs. The label-capture-release process of CTCs is validated for the first time, and our study opens new avenues for downstream CTC applications beyond simple enumeration.

DATA AND CODE AVAILABILITY

The data and code supporting the findings of this study are available within the paper.

REFERENCES

1. Plaks, V., Koopman, C.D., and Werb, Z. (2013). Cancer. Circulating tumor cells. Science ***341***: 1186–1188.
2. Chaffer, C.L., and Weinberg, R.A. (2011). A perspective on cancer cell metastasis. Science ***331***: 1559–1564.

3. Nagrath, S., Sequist, L.V., Maheswaran, S., et al. (2007). Isolation of rare circulating tumour cells in cancer patients by microchip technology. Nature ***450***: 1235–1239.
4. Tamminga, M., Andree, K.C., Hiltermann, T.J.N., et al. (2020). Detection of circulating tumor cells in the diagnostic leukapheresis product of non-small-cell lung cancer patients comparing CellSearch® and ISET. Cancers ***12***: 896.
5. Zeng, H., Veeramootoo, J.S., Ma, G., et al. (2020). Clinical value and feasibility of ISET in detecting circulating tumor cells in early breast cancer. Transl. Cancer Res. ***9***: 4297–4305.
6. Werbin, J.L., Nordberg, J.J., Tzucker, J., et al. (2017). RareCyte® CTC analysis step 2: Detection of circulating tumor cells by CyteFinder® automated scanning and semiautomated image analysis. Methods Mol. Biol. ***1634***: 173–180.
7. Ramirez, A.B., U'Ren, L., Campton, D.E., et al. (2017). RareCyte® CTC analysis step 1: AccuCyte® sample preparation for the comprehensive recovery of nucleated cells from whole blood. Methods Mol. Biol. ***1634***: 163–172.
8. Descamps, L., Le Roy, D., and Deman, A.L. (2022). Microfluidic-based technologies for CTC isolation: A review of 10 years of intense efforts towards liquid biopsy. Int. J. Mol. Sci. ***23***: 1981.
9. Wong, A.H.H. (2023). Pushing the boundary of cancer diagnostics through microfluidic technologies. Innovat. Med. ***1***: 100005.
10. Andree, K.C., Barradas, A.M.C., Nguyen, A.T., et al. (2016). Capture of tumor cells on anti-EpCAM-functionalized poly(acrylic acid)-coated surfaces. ACS Appl. Mater. Interfaces ***8***: 14349–14356.
11. Myung, J.H., Launiere, C.A., Eddington, D.T., et al. (2010). Enhanced tumor cell isolation by a biomimetic combination of E-selectin and anti-EpCAM: implications for the effective separation of circulating tumor cells (CTCs). Langmuir ***26***: 8589–8596.
12. Wu, L., Wang, Y., Xu, X., et al. (2021). Aptamer-based detection of circulating targets for precision medicine. Chem. Rev. ***121***: 12035–12105.
13. Radisky, D.C. (2005). Epithelial-mesenchymal transition. J. Cell Sci. ***118***: 4325–4326.
14. Saez, J., Garcia-Hernando, M., Savva, A., et al. (2023). Capture and release of cancer cells through smart bioelectronics. Methods Mol. Biol. ***2679***: 305–314.
15. Zhao, W., Cui, C.H., Bose, S., et al. (2012). Bioinspired multivalent DNA network for capture and release of cells. Proc. Natl. Acad. Sci. USA ***109***: 19626–19631.
16. Rupp, B., Ball, H., Wuchu, F., et al. (2022). Circulating tumor cells in precision medicine: challenges and opportunities. Trends Pharmacol. Sci. ***43***: 378–391.
17. Cheng, S.B., Wang, M., Zhang, C., et al. (2020). Flexible three-dimensional net for intravascular fishing of circulating tumor cells. Anal. Chem. ***92***: 5447–5455.
18. Mohamadi, R.M., Besant, J.D., Mepham, A., et al. (2015). Nanoparticle-mediated binning and profiling of heterogeneous circulating tumor cell subpopulations. Angew. Chem. Int. Ed. ***54***: 139–143.
19. Powell, A.A., Talasaz, A.H., Zhang, H., et al. (2012). Single cell profiling of circulating tumor cells: transcriptional heterogeneity and diversity from breast cancer cell lines. PLoS One ***7***: e33788.
20. Martinez-Outschoorn, U.E., Peiris-Pagés, M., Pestell, R.G., et al. (2017). Cancer metabolism: a therapeutic perspective. Nat. Rev. Clin. Oncol. ***14***: 11–31.
21. Cairns, R.A., Harris, I.S., and Mak, T.W. (2011). Regulation of cancer cell metabolism. Nat. Rev. Cancer ***11***: 85–95.
22. Sletten, E.M., and Bertozzi, C.R. (2009). Bioorthogonal chemistry: fishing for selectivity in a sea of functionality. Angew. Chem. Int. Ed. ***48***: 6974–6998.
23. Wratil, P.R., Horstkorte, R., and Reutter, W. (2016). Metabolic glycoengineering with N-acyl side chain modified mannosamines. Angew. Chem. Int. Ed. ***55***: 9482–9512.
24. Agatemor, C., Buettner, M.J., Ariss, R., et al. (2019). Exploiting metabolic glycoengineering to advance healthcare. Nat. Rev. Chem ***3***: 605–620.
25. Chen, X., Li, X., He, W., et al. (2023). Rational multivalency construction enables bactericidal effect amplification and dynamic biomaterial design. Innovation ***4***: 100483.
26. Du, Z., Qiao, F., Tong, L., et al. (2024). Mimicking Mytilus edulis foot protein: A versatile strategy for robust biomedical coatings. Innovation ***5***: 100671.
27. Du, J., Meledeo, M.A., Wang, Z., et al. (2009). Metabolic glycoengineering: sialic acid and beyond. Glycobiology ***19***: 1382–1401.
28. Saxon, E., and Bertozzi, C.R. (2000). Cell surface engineering by a modified Staudinger reaction. Science ***287***: 2007–2010.
29. Prescher, J.A., Dube, D.H., and Bertozzi, C.R. (2004). Chemical remodelling of cell surfaces in living animals. Nature ***430***: 873–877.
30. Yoon, H.Y., Lee, D., Lim, D.K., et al. (2022). Copper-free click chemistry: Applications in drug delivery, cell tracking, and tissue engineering. Adv. Mater. ***34***: e2107192.
31. Mthembu, S.N., Sharma, A., Albericio, F., et al. (2020). Breaking a couple: disulfide reducing agents. Chembiochem ***21***: 1947–1954.
32. Roseman, S., Jourdian, G.W., Watson, D., et al. (1961). Enzymatic synthesis of sialic acid 9-phosphates. Proc. Natl. Acad. Sci. USA ***47***: 958–961.
33. Pouilly, S., Piller, V., and Piller, F. (2012). Metabolic glycoengineering through the mammalian GalNAc salvage pathway. FEBS J. ***279***: 586–598.
34. Keeley, T., Lin, S., Lester, D.K., et al. (2018). The fucose salvage pathway inhibits invadopodia formation and extracellular matrix degradation in melanoma cells. PLoS One ***13***: e0199128.
35. Mbua, N.E., Guo, J., Wolfert, M.A., et al. (2011). Strain-promoted alkyne-azide cycloadditions (SPAAC) reveal new features of glycoconjugate biosynthesis. Chembiochem ***12***: 1912–1921.
36. Lin, D., Shen, L., Luo, M., et al. (2021). Circulating tumor cells: biology and clinical significance. Signal Transduct. Targeted Ther. ***6***: 404.
37. Li, R., Chen, F.F., Liu, H.Q., et al. (2018). Efficient capture and high activity release of circulating tumor cells by using TiO2 nanorod arrays coated with soluble MnO2 nanoparticles. ACS Appl. Mater. Interfaces ***10***: 16327–16334.
38. Xiao, Y., Wang, M., Lin, L., et al. (2019). Specific capture and release of circulating tumor cells using a multifunctional nanofiber-integrated microfluidic chip. Nanomedicine ***14***: 183–199.
39. Li, Y., Lu, Q., Liu, H., et al. (2015). Antibody-modified reduced graphene oxide films with extreme sensitivity to circulating tumor cells. Adv. Mater. ***27***: 6848–6854.
40. Xu, Y., Li, Y., Gao, A., et al. (2023). Gasotransmitter delivery for bone diseases and regeneration. Innov. Life ***1***: 100015.
41. Muxika, A., Etxabide, A., Uranga, J., et al. (2017). Chitosan as a bioactive polymer: Processing, properties and applications. Int. J. Biol. Macromol. ***105***: 1358–1368.
42. Sun, N., Liu, M., Wang, J., et al. (2016). Chitosan nanofibers for specific capture and nondestructive release of CTCs assisted by pCBMA brushes. Small ***12***: 5090–5097.
43. Wang, Z., Wu, Z., Ding, P., et al. (2021). Selective capture of circulating tumor cells by antifouling nanostructure substrate made of hydrogel nanoparticles. Colloids Surf. B Biointerfaces ***202***: 111669.
44. Holthöfer, H.A., Miettinen, A., Paasivuo, R., et al. (1983). Fluorescence microscopic study with kidney-specific antibodies, antiintermediate filament antibodies, and lectins. Lab. Invest. ***49***: 317.
45. Yu, M., Bardia, A., Aceto, N., et al. (2014). Cancer therapy. Ex vivo culture of circulating breast tumor cells for individualized testing of drug susceptibility. Science ***345***: 216–220.
46. Smit, D.J., Pantel, K., and Jücker, M. (2021). Circulating tumor cells as a promising target for individualized drug susceptibility tests in cancer therapy. Biochem. Pharmacol. ***188***: 114589.
47. Bhimani, J., O'Connell, K., Persaud, S., et al. (2024). The landscape of use of NCCN-guideline chemotherapy regimens in stage I-IIIA breast cancer in an integrated healthcare delivery system. Breast Cancer Res. Treat. ***208***: 405–414.

ACKNOWLEDGMENTS

This work was financially supported by the National Key R&D Program of China (2021YFB3800800), the National Natural Science Foundation of China (81903057, 82073284, 32000962, 82402491, and 82272157), Shenzhen Science and Technology Research Funding (JCYJ20200109115601720), the Hong Kong PDFS-RGC Postdoctoral Fellowship Scheme (PDFS2122-1S08 and CityU 9061014), as well as Hong Kong HMRF (Health and Medical Research Fund) (2120972 and CityU 9211320). We also acknowledge helpful discussions with Dr. Ya Zhao, Dr. Guofen Song, Dr. Ang Gao, and Dr. Shi Mo. Moreover, we acknowledge helpful technical support from Dr. Xiaoyu Pu from Xingyuan Co. Ltd. (China). The funders had no role in study design, data collection and analysis, decision to publish, or preparation of the manuscript.

AUTHOR CONTRIBUTIONS

Z.L. performed the chemical synthesis and material preparation experiment; Z.L., X.R., and L.X. performed the cell experiments; and Y. Z. collected clinical blood samples. Z.L. and D.Z. performed the clinical tests; Z.L., X.R., P.L., and L.T. analyzed the data; W.L., Y.C., and H.W. contributed to the theoretical interpretation of the data; and Z.L., X.R., W.L., P.K.C., and H.W. wrote the manuscript with comments from all co-authors. Z.L., W.L., Y.C., and H.W. conceived and supervised the project. All authors contributed to the manuscript and approved the final version.

DECLARATION OF INTERESTS

The authors declare no competing interests.

SUPPLEMENTAL INFORMATION

It can be found online at https://doi.org/10.1016/j.xinn.2025.100805.

The Innovation, Volume *6*

Supplemental Information

A phenotype-independent "label-capture-release" process for isolating viable circulating tumor cells in real-time drug susceptibility testing

Zhiqi Lao, Xiaoxue Ren, Dehua Zhuang, Lingxia Xie, Yucong Zhang, Wei Li, Yue Chen, Penghui Li, Liping Tong, Paul K. Chu, and Huaiyu Wang

Materials and Methods

Ethanol, methanol, dichloromethane, ethyl acetate, petroleum ether, pyridine, acetonitrile, *N,N*-dimethylformamide, triethylamine, D-mannosamine hydrochloride, cystamine dihydrochloride, trifluoroacetate, acetic anhydride, 4-dimethylaminopyridine (DMAP), sulfobetaine methacrylate (SBMA), methacrylic acid (MAA), *N, N'*-methylenebisacrylamide (MBA), 2,2-azobisisobutyronitrile (AIBN), 1-ethyl-3-(3′-dimethylaminopropyl) carbodiimide (EDC), *N*-hydroxysuccinimide (NHS), 4',6-Diamidino-2'phenylindole (DAPI), bovine serum albumin (BSA), and Histopaque-1077 solution were obtained from Sigma-Aldrich (USA).

Chemical synthesis of Ac_4ManNAc, Ac_4ManNAz and DBCO-SS-NH_2

The synthesis of Ac_4ManNAc and Ac_4ManNAz was according to a previously reported method.[48]

Ac_4ManNAc: D-Mannosamine hydrochloride (215.63 mg, 1.00 mmol) was added to a flask containing pyridine (10 mL), acetic anhydride (1.02 g, 10.00 mmol), and DMAP (12.22 mg, 0.10 mmol). The mixture was stirred overnight, concentrated by rotary evaporation, and purified by column chromatography (ethyl acetate: petroleum ether = 1:1) to produce Ac_4ManNAc (378.63 mg, 0.97 mmol, 97%) as a white solid.

Ac_4ManNAz: A mixture of D-mannosamine hydrochloride (215.63 mg, 1.00 mmol), EDC (383.40 mg, 2.00 mmol), NHS (172.63 mg, 1.50 mmol) and triethylamine (0.5 mL) was stirred in methanol (10 mL). Azido acetic acid (121.27 mg, 1.20 mmol) was added and the mixture was stirred overnight, concentrated by rotary evaporation, and purified by column chromatography (methanol: dichloromethane = 5:1) to yield ManNAz (120.62 mg, 0.46 mmol, 46%) as a white solid. ManNAz (120.62 mg, 0.46 mmol) was added to a flask containing pyridine (5 mL), acetic anhydride (0.51 g, 5.00 mmol) and DMAP (6.11 mg, 0.05 mmol). The mixture was stirred overnight, concentrated

by rotary evaporation, and purified by column chromatography (ethyl acetate: petroleum ether = 1:1) to produce Ac_4ManNAz (189.36 mg, 0.44 mmol, 96%) as a white solid.

DBCO-SS-NH_2: Di-tert-butyl decarbonate (2.18 g, 5.00 mmol) was added slowly to a *N,N*-dimethylformamide solution (20 mL) containing cystamine dihydrochloride (2.25 g, 10.00 mmol) and triethylamine (5 mL). The mixture was stirred overnight, concentrated by rotary evaporation, and purified by column chromatography (methanol: dichloromethane = 10:1) to produce cystamine mono-Boc ester (1.09 g, 4.31 mmol, 86%). A mixture of DBCO-NHS (402.40 mg, 1.00 mmol) and cystamine mono-Boc ester (252.40 mg, 1.00 mmol) was stirred in dichloromethane for 6 hours and purified by column chromatography (ethyl acetate: petroleum ether = 1:2) to produce DBCO-SS-NHBoc (539.72 mg, 0.92 mmol, 92%) as a white solid. DBCO-SS-NHBoc (539.72 mg, 0.92 mmol) was treated with trifluoroacetate (1 mL) in dichloromethane (10 mL). DBCO-SS-NH_2 (87.92 mg, 0.20 mmol, 22%) white solid was obtained after solvent evaporation and then purified by column chromatography (methanol: dichloromethane = 4:1).

MGE experiments

Cell culture: The human small cell lung cancer cell line (H524, suspended), human T-lymphoblastic cancer cell line (Jurkat, suspended), human cervical cancer cell line (HeLa), human non-small cell lung cancer cell line (A549), human hepatocellular carcinomas cell lines (HepG2 and Huh-7), and human breast cancer cell lines (MCF-7 and MCF-7 DR) were used in the cell experiments. MCF-7 DR cells were obtained from Zhong Qiao Xin Zhou Co. Ltd. (China), and all the other cell strains were obtained from the Cell Bank of the Chinese Academy of Sciences. The H524 cells, MCF-7 cells, A549 cells, HeLa cells, and HepG2 cells were cultured by Dulbecco's modified eagle medium (DMEM) supplemented with 10% (v/v) fetal bovine serum (FBS) and 1%

(w/v) penicillin/streptomycin. Jurkat cells and H716 cells were cultured in the RPMI-1640 medium with 10% (v/v) FBS and 1% (w/v) penicillin/streptomycin. Huh-7 cells were cultured in DMEM with 10% (v/v) FBS and 1% (w/v) penicillin/streptomycin+$NaHCO_3$. MCF-7 DR cells were cultured in DMEM with 10% (v/v) FBS and 1% (w/v) penicillin/streptomycin+DOX (250 ng/mL). PBMCs were cultured in the serum-free lymphocyte culture medium (Stemcell®).

MGE conditions in cell culture: Ac_4ManNAz, Ac_4ManNAc and DBCO-biotin were dissolved in DMSO at a concentration of 100 mM and stored at -20 ºC. The solution was warmed to room temperature and added to cell culture medium with a certain concentration before use. The cancer cells were sub-cultured for at least 3 generations before use. The PBMCs were separated from fresh healthy blood by the Histopaque-1077 solution and SepMate™-15 centrifuge tube according to manufacturer's instruction.

MGE procedures: The cancer cells were seeded at a density of 0.3-0.4 million cells per mL in 4 mL of culture medium. During cell culturing, Ac_4ManNAz or Ac_4ManNAc was added for a certain time to allow metabolic incorporation of *N*-azidoacetyl sialic acid to the glycoproteins of the cells. The PBMCs separated from 1 mL of fresh blood were seeded in 15 mL of the culture medium and incubated with Ac_4ManNAz or Ac_4ManNAc under the same conditions.

Cell Viability: The cells were seeded at a density of 0.3 million cells per mL in 4 mL of the culture medium with/without addition of Ac_4ManNAz (100 μM). After 12 hours, the number of cells was counted and the cell viability was calculated as the number of cells with Ac_4ManNAz divided by the number of cells without Ac_4ManNAz. Data were collected from 3 parallel tests.

Specific fluorescent staining of azido groups: Around 10000 cells with/without azido groups were washed with the labeling buffer (PBS solution with 2% FBS) and suspended in a tube or seeded onto a cell crawling sheet. The cells were incubated with DBCO-biotin (100 μM, 1 hour) in the

labeling buffer at room temperature, washed 3 times with the labeling buffer (each time at least 10 minutes), and then incubated with Alexa Fluor 488-labeled streptavidin (50 μM, 15 minutes) in the dark. After fluorescent staining, the suspended cells were placed on a glass slide and the cells on the crawling sheet were used directly. All the cells were co-stained by DAPI (10 μg/mL, 3 minutes), and the relative fluorescence intensity for each individual cell was monitored by automatic scanning fluorescence microscopy (Axio Imager Z2, Zeiss, Germany). Data points were collected in triplicate from 3 separate experiments.

Fabrication of multi-functional bio-orthogonal films

CF: Chitosan (200 mg, MW = 200,000) was dissolved in 10 mL of 90% acetic acid. After the chitosan solution (70 μL) was added to a round glass slide (d = 14 mm), the film was prepared by spin coating at 4,000 revolutions per minute (rpm) for 15 seconds. The film was dried at 60 ºC for 24 hours, and 1 M NaOH was added to expose the active amino groups on the surface. The film was dried at 60 ºC for 24 hours to produce CF.

CF-DBCO: CF was modified by 10 mM DBCO-NHS in ethanol overnight. The surface was washed with ethanol 3 times and PBS 3 times to produce CF-DBCO and then stored at 4 ºC in darkness.

Anti-fouling nanoparticles: The antifouling nanoparticles were prepared according to a modified protocol.[43] SBMA (1.00 g, 3.58 mmol), MAA (0.10 g, 1.16 mmol), MBA (0.10 g, 0.65 mmol), and AIBN (20.00 mg, 0.12 mmol) were added to acetonitrile (100 mL) and the mixture was heated to 110 ºC for 30 minutes. After cooling to room temperature, the white nanoparticles were collected and washed with ethanol and water, centrifuged, and stored at 4 ºC.

CF-NP-DBCO: The nanoparticles were activated by 0.1 M EDC and 0.05 M NHS for 30 minutes and then added to CF. After 12 hours, the surface was washed with a mixture of ethanol/water 3 times and double-distilled water 3 times to remove uncombined nanoparticles and produce CF-NP-COOH (partly CF-NP-CO-NHS ester). The surface was re-activated by 0.1 M EDC and 0.05 M NHS for 30 minutes to make sure all the surface carboxyl groups were converted into NHS ester. Subsequently, DBCO-NH_2 in DMSO (10 mM) was added slowly, shaken for 12 hours in the dark, and washed with ethanol/water 3 times and double-distilled water 3 times to produce CF-NP-DBCO. The CF-NP-DBCO films were stored at 4 ºC in darkness.

CF-NP-SS-DBCO: CF-NP-COOH was re-activated by 0.1 M EDC and 0.05 M NHS for 30 minutes to make sure all the surface carboxyl groups were converted into NHS ester. Afterward, DBCO-SS-NH_2 in DMSO (10 mM) was added slowly, shaken for 12 hours in darkness, and washed with ethanol/water 3 times and double-distilled water 3 times to produce CF-NP-SS-DBCO. The CF-NP-SS-DBCO films were stored at 4 ºC in darkness.

Characterization of bio-orthogonal films

Surface morphologies and chemical structures: The surface morphologies of the CF-DBCO, CF-NP-DBCO, and CF-NP-SS-DBCO films were observed by SEM (SUPRA^{TM} 55, Carl Zeiss, Germany) and the chemical structures were determined by XPS (ESCALab250Xi, Thermo Fisher Scientific, USA) and EDS (X-Max, Oxford Instruments, UK).

Capturing selectivity of azido-positive and azido-negative cancer cells: The cells were seeded at a density of 0.3~0.4 million cells per mL in 4 mL of the culture medium. During cell culturing, Ac_4ManNAz (100 μM) or Ac_4ManNAc (100 μM) was added for 12 hours to allow metabolic incorporation of *N*-azidoacetyl sialic acid onto the glycoproteins of the cells. The treated cells were

collected by centrifugation and washed by PBS for 3 times. Next, the bio-orthogonal films on a 24-well plate were added with 50000 cells in 1 mL of PBS and shaken at a speed of 20 rpm for 1 hour. The samples were rinsed with PBS at least 5 times and the captured cells were stained by DAPI (10 μg/mL, 3 minutes) and examined by fluorescent microscopy (BX51, Olympus Corporation, Japan) with 3 different views. Data points were collected in triplicate from 3 separate experiments and the capturing rate was calculated as the number of captured cells divided by 50000.

Capturing selectivity of azido-positive cancer cells and PBMCs: The H524 cells were seeded at a density of 0.2~0.3 million cells per mL in 4 mL of the culture medium and the PBMCs separated from 1 mL of fresh blood were seeded in 15 mL of the culture medium. During cell culturing, Ac_4ManNAz (100 μM) was added for 12 hours to allow metabolic incorporation of *N*-azidoacetyl sialic acid onto the glycoproteins of the cells. The treated cancer cells and PBMCs were separately collected by centrifugation and washed with PBS 3 times. Afterward, both kinds of cell suspensions (50000 H524 cells in 1 mL of PBS and 4~8 million PBMCs in 1 mL of PBS) were prepared, added onto the bio-orthogonal films on a 24-well plate respectively, and then shaken at a speed of 20 rpm for 1 hour. The samples were rinsed with PBS at least 5 times and the captured cells were stained by DAPI (10 μg/mL, 3 minutes) and examined by fluorescent microscopy (BX51, Olympus Corporation, Japan) with 3 different views. Data points were collected in triplicate from 3 separate experiments. The capturing rate was calculated as the number of captured cells divided by 50000 and that of PBMCs was calculated as the number of captured PBMCs divided by the number of PBMCs counted before capturing.

Release of the captured cancer cells: The cancer cells captured by the CF-NP-DBCO and CF-NP-SS-DBCO films underwent DAPI (10 μg/mL, 3 minutes) staining and examined by fluorescence

138 microscopy. Dithiothreitol (DTT, 10 mM) in culture medium was added to mediate disulfide
139 reduction and release the captured cells. To ensure a sufficient reaction, the DTT solution was
140 shaken at 80 rpm for 40 minutes and then the sample was washed gently with 2~3 mL of PBS at
141 least 5 times. The released cells were concentrated by centrifugation and re-suspended in 1 mL of
142 PBS. 20 μL of the cell suspension were added to a glass slide and stained by DAPI (10 μg/mL, 3
143 minutes) to count the cell number. The released cells were further subjected to Calcein-
144 AM/Propidium iodide staining (100 μM, 30 minutes) to evaluate the viability. Data points were
145 collected in triplicate from 3 separate experiments. The release rate was calculated as the number
146 of released cells divided by the number of cells counted after capturing. The cell survival rate was
147 calculated as the number of alive cells divided by the total number of released cells. For the
148 evaluation of long-term cell viability, both the released cells and normal cells were added onto a
149 24-well plate at a density of 100000 per well and cultured for 1 and 3 days. At each time point,
150 CCK-8 assay was performed according to manufacturer's instruction. The long-term cell viability
151 was calculated as the CCK-8 testing result at Day 3 divided by the CCK-8 testing result at Day 1.
152 *Comparison of capturing capability between ISET and bio-orthogonal films:* 10000 HeLa or H524
153 cells were dispersed in 10 mL of PBS, and then purified by the ISET standard membrane according
154 to manufacturer's instruction. As for the bio-orthogonal capture, 10000 HeLa or H524 cells labeled
155 by Ac_4ManNAz were dispersed in 1 mL of PBS, added onto the bio-orthogonal films on a 24-well
156 plate, and then shaken at a speed of 20 rpm for 1 hour, followed by PBS washing at least 5 times.
157 Data points were collected in triplicate and the capturing rate was calculated as the number of
158 captured cells divided by 10000.
159 *Capture of artificial CTCs in blood samples:* 10000 HeLa or H524 cells were dispersed in 1 mL
160 of PBS, and 10 μL of the cell suspensions were added into 1 mL of fresh blood separately for the

preparation of artificial CTCs. Each sample was pretreated with the ACK lysis buffer at 0 ºC for 10 minutes and collected by centrifugation under 300 g. After washing with PBS containing 2% FBS, the remaining cells were cultured in the serum-free lymphocyte culture medium containing 100 μM Ac_4ManNAz for 12 hours. The treated cells were washed with PBS 3 times, added to CF-NP-DBCO on a 24-well plate, and shaken at 20 rpm for 1 hour. The samples were rinsed with PBS at least 5 times and the cells were fixed by 4% paraformaldehyde and Triton X-100 (0.1% in H_2O, 5 minutes). Finally, the fixed cells were treated with a mixture of Alexa Fluor 594-labeled pan-CK probe (50 μM, 15 minutes), Alexa Fluor 750-labeled CD45 probe (50 μM, 15 minutes), and DAPI (10 μg/mL, 15 minutes). An automatic scanning fluorescent microscope (Axio Imager Z2, Zeiss, Germany) was used to identify the captured cancer cells as the Nucleus+/CD45-/pan-CK+. The data were collected 9 times for each cell line, and the capturing rate was calculated as the number of captured cancer cells divided by 100.

Clinical CTCs detection

Cells isolated by ISET and identified by nucleus/CD45/clinical-marker/azido staining: The ethylenediaminetetraacetic acid (EDTA) anticoagulated whole blood samples were obtained from different cancer patients in Shenzhen People's Hospital. Each blood sample was pretreated with ACK lysis buffer at 0 ºC for 10 minutes and purified by the ISET standard membrane according to the manufacturer's instructions. The cells remaining on the ISET membrane were cultured in the serum-free lymphocyte culture medium containing 100 μM Ac_4ManNAz for 12 hours. Afterward, the membrane was washed with PBS 5 times, and the cells were fixed by 4% paraformaldehyde. The fixed cells were treated with DBCO-biotin (100 μM, 1 hour), Alexa Fluor 488-labeled streptavidin (50 μM, 15 minutes), Triton X-100 (0.1% in H_2O, 5 minutes), respectively.

After careful washing, the remaining cells were further treated by a mixture of Alexa Fluor 594-labeled pan-CK probe (50 μM, 15 minutes) or Alexa Fluor 594-labeled EpCAM-CKs probe (50 μM, 15 minutes) and DAPI (10 μg/mL, 15 minutes). Finally, the cells were treated with an Alexa Fluor 750-labeled CD45 gene probe (100 μM, 3 hours). An automatic scanning fluorescent microscope (Axio Imager Z2, Zeiss, Germany) was used to identify CTCs as Nucleus+/CD45-/Clinical marker+.

Direct comparison between our technique and TumorFisher® detection system: The EDTA anticoagulated whole blood samples were obtained from different cancer patients in Shenzhen People's Hospital as well as healthy people. Each blood sample was halved and parallelly processed by TumorFisher® and our workflow as described above. Afterward, all the CTCs captured by different systems underwent immunohistochemical staining.

Fluorescence labeling of azide and thiol groups: The MCF-7 or MCF-7 DR cells were seeded with a density of 0.3-0.4 million cells per mL in 4 mL of culture medium with/without the addition of Ac_4ManNAz (100 μM). After culturing for 12 hours, the cells were harvested, incubated with DBCO-biotin (100 μM, 1 hour) and/or MAM-biotin (200 μM, 1 hour) in the labeling buffer at room temperature, washed 3 times with the labeling buffer (each time at least 10 minutes), and then incubated with Alexa Fluor 488-labeled streptavidin (50 μM, 15 minutes) in the dark. Subsequently, the medium (20 μL) was added to the confocal dish with a 3 mm x 3 mm hole and observed under a confocal microscope (STEDYCON, Leica, Germany). The total fluorescence intensity (FI) of Alexa Fluor 488 and area (S) were examined on 40 randomly selected cells using ImageJ software, and the relative fluorescence intensity (RFI) was calculated by the formula: RFI=FI/{2π [(S/π)^0.5]}. Data points were collected in triplicate from 3 separate experiments.

206 *Evaluation of cell viability based on MGE:* The MCF-7 or MCF-7 DR cells were seeded with a
207 density of 0.3-0.4 million cells per mL in 4 mL of the culture medium. During cell culturing,
208 Ac_4ManNAz (100 μM) was added together with DOX, CDDP, or PTX at certain concentrations.
209 After 24 hours, the cells were harvested, incubated with DBCO-biotin (100 μM, 1 hour) and
210 MAM-biotin (200 μM, 1 hour) in the labeling buffer at room temperature, washed 3 times with
211 the labeling buffer (each time at least 10 minutes), and then incubated with Alexa Fluor 488-
212 labeled streptavidin (50 μM, 15 minutes) in the dark. Subsequently, the medium (20 μL) was added
213 to the confocal dish with a 3 mm x 3 mm hole and observed under a confocal microscope
214 (STEDYCON, Leica, Germany). The relative fluorescence intensity of Alexa Fluor 488 was
215 examined by examining 40 randomly selected cells, as mentioned above. Data points were
216 collected in triplicate from 3 separate experiments. The drug sensitivity was characterized by the
217 ratio of relative fluorescence intensity between the experimental group and the control group. For
218 standard reference, the cells treated with different drugs are examined by the CCK-8 assay
219 according to the manufacturer's instructions.
220 *Drug susceptibility tests using artificial CTCs*: 10000 MCF-7 or MCF-7 DR cells were dispersed
221 in 1 mL of PBS, and 50 μL of the cell suspensions were added into 20 mL of fresh blood separately
222 for the preparation of artificial CTCs. Each blood sample was pretreated with the ACK lysis buffer
223 at 0 ºC for 10 minutes and collected by centrifugation under 300 g. After washing with PBS
224 containing 2% FBS, the remaining cells were evenly divided into 4 potions, and then cultured in
225 the serum-free lymphocyte culture medium containing Ac_4ManNAz (100 μM) and different drugs
226 at a concentration of IC_{35} for 24 hours. Subsequently, the treated cells were processed by our
227 capture-release workflow using CF-NP-SS-DBCO films as described above. The released cells
228 were incubated with DBCO-biotin (100 μM, 1 hour) and MAM-biotin (200 μM, 1 hour) in the

labeling buffer at room temperature, washed 3 times with the labeling buffer (each time at least 10 minutes), and then incubated with a mixture of Hoechst-33342 (10 μM, 15 minutes)/Alexa Fluor 488-labeled streptavidin (50 μM, 15 minutes)/Alexa Fluor 647-labeled CD45 (50 μM, 15 minutes)/Alexa Fluor 594-labeled EpCAM-CKs (50 μM, 15 minutes) in the dark. After fluorescent staining, the medium (20 μL) was added to the confocal dish with a 3 mm x 3 mm hole and observed under a confocal microscope (STEDYCON, Leica, Germany). The artificial CTCs were identified as Nucleus+/CD45-/EpCAM+, and their relative fluorescence intensity of Alexa Fluor 488 was examined as mentioned above. The drug sensitivity was characterized by the ratio of relative fluorescence intensity between the experimental group and the control group.

Statistical analysis

The cell experiments were performed at least in triplicate with the results being presented as mean + standard deviation. The student's *t-test* was performed to determine the levels of statistical significance among different groups. A difference of $*p < 0.05$ was considered to be significant, and that of $**p < 0.01$ or $***p < 0.001$ was considered to be highly significant.

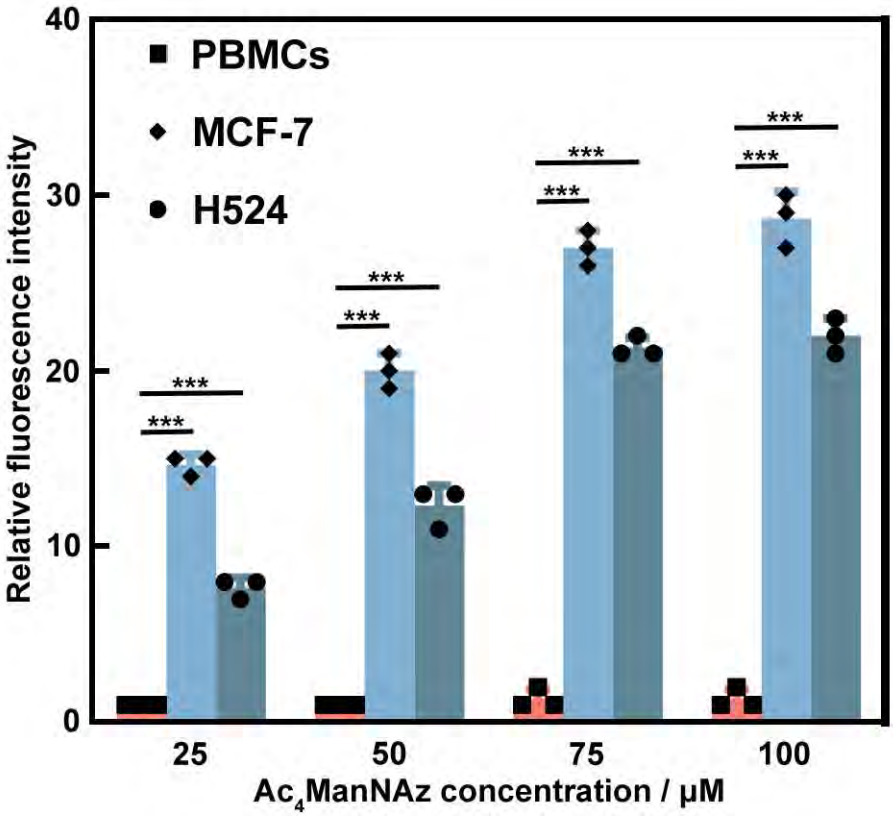

Supplementary Figure 1. Sugar concentration-cell surface fluorescence intensity histograms (*** denotes $p < 0.001$).

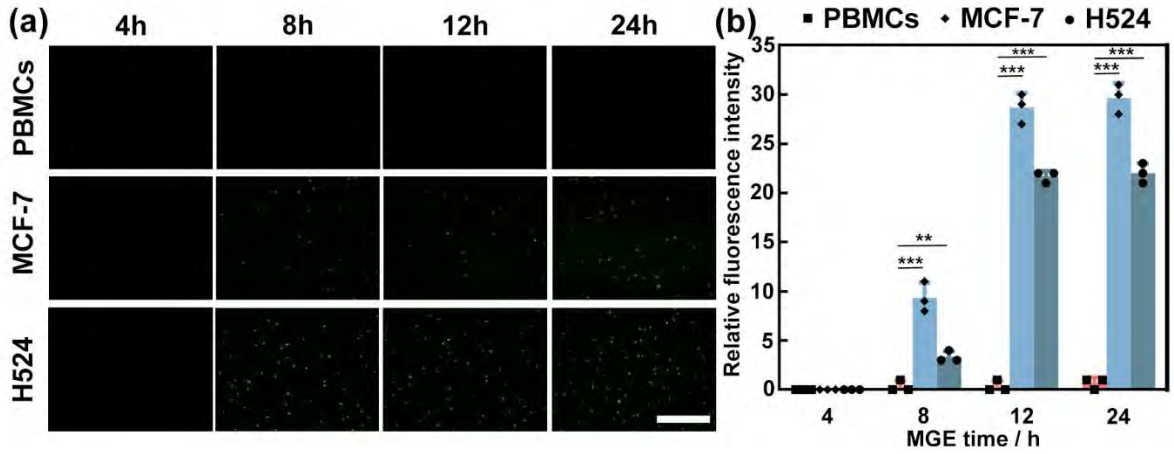

Supplementary Figure 2. (a) Fluorescent images of different cells for different MGE times (scale bar = 200 μm); (b) MGE time-cell surface fluorescence intensity histograms (** denotes $p < 0.01$ and *** denotes $p < 0.001$).

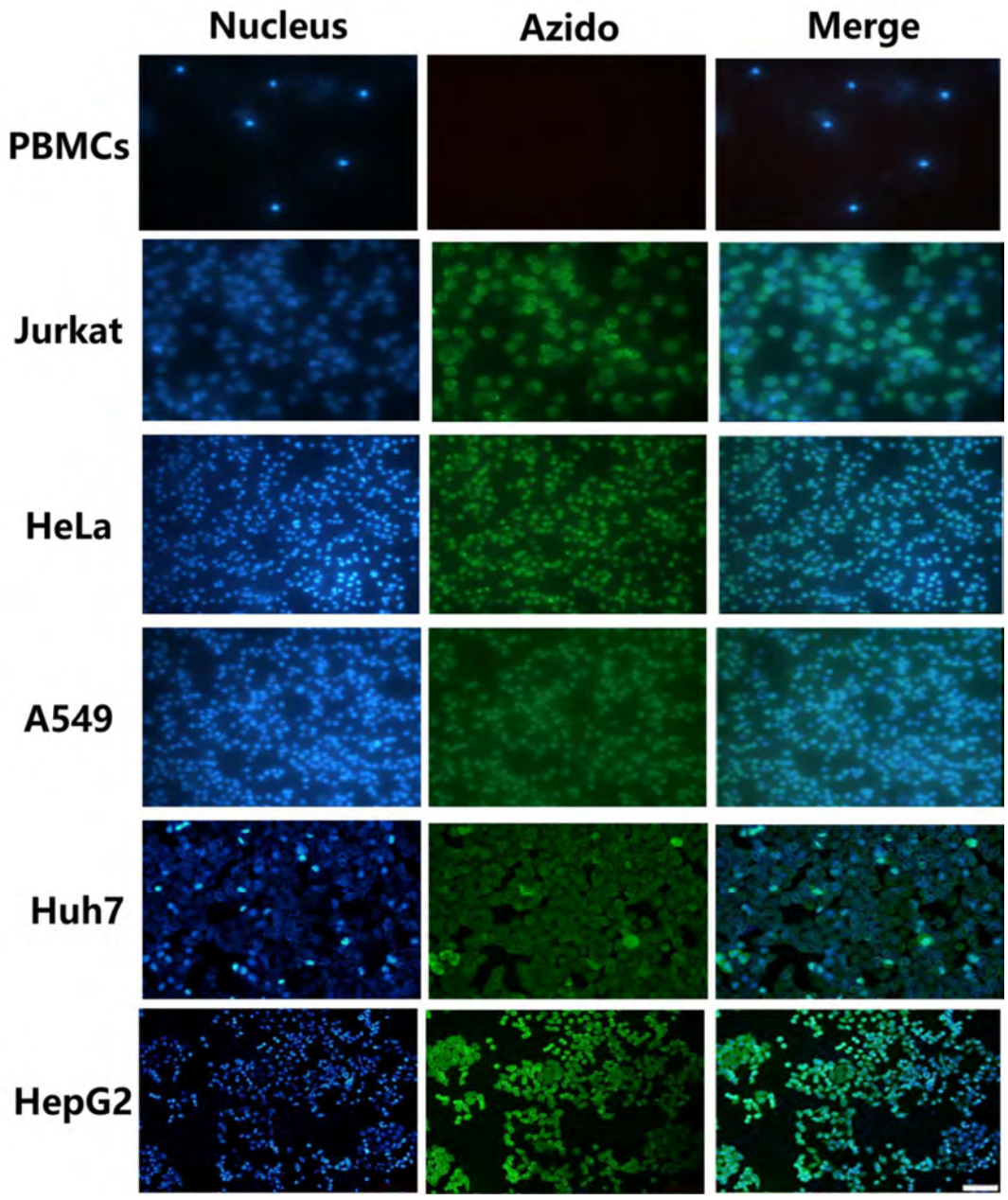

Supplementary Figure 3. Fluorescent images of MGE-labeled cancer cells and PBMCs (scale bar = 200 μm) showing that the cancer cells are selectively modified by MGE while normal blood cells are not.

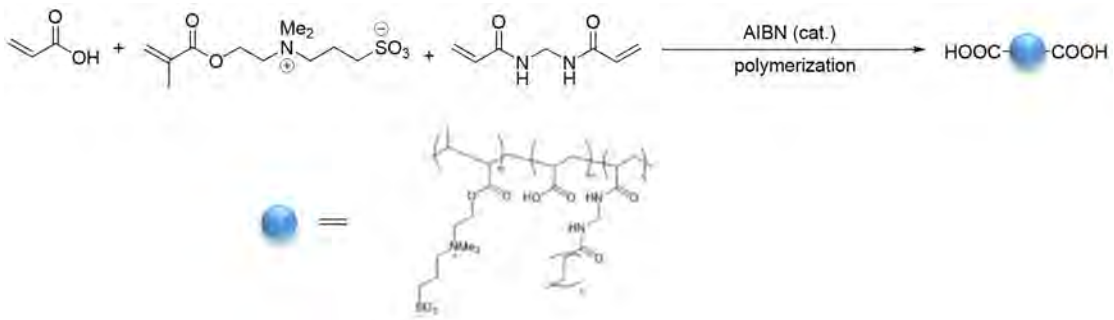

Supplementary Figure 4. Synthesis of anti-fouling nanoparticles.

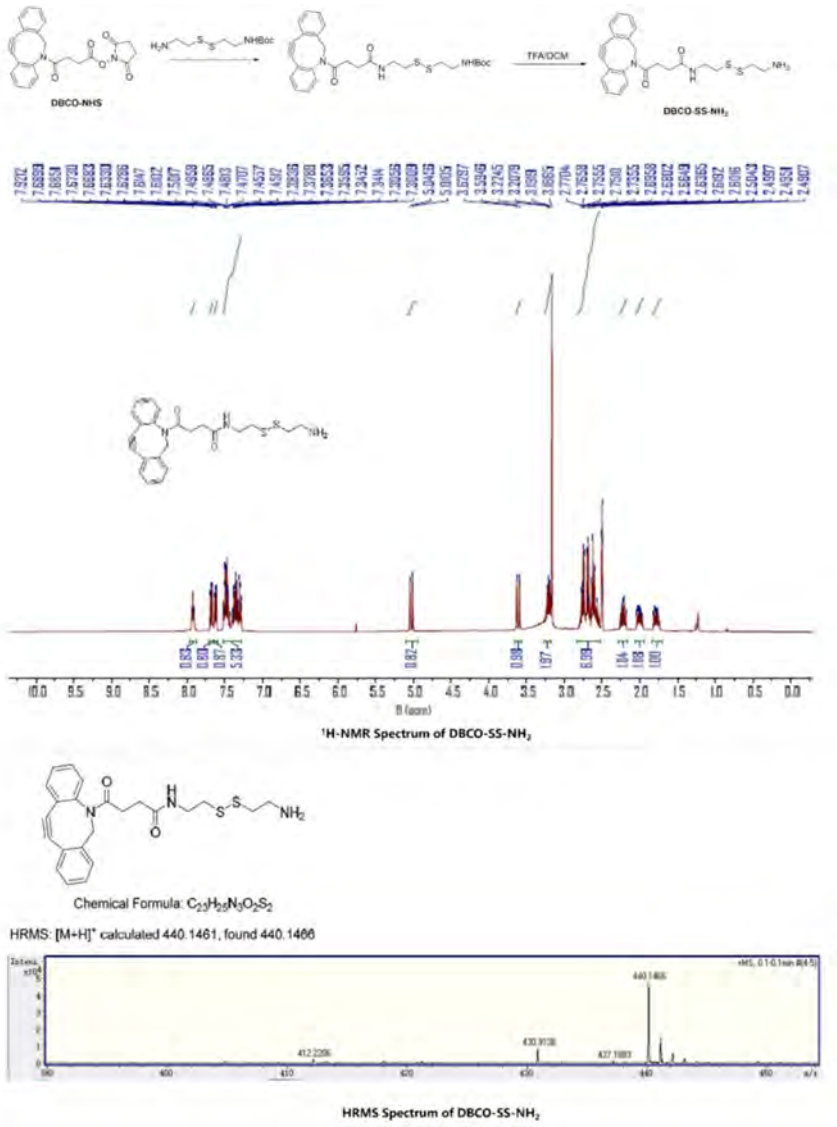

Supplementary Figure 5. Synthesis and characterization of DBCO-SS-NH_2: ^{1}H NMR (400 MHz, dimethylsulfoxide-d6) δ 7.91 (1H, t), 7.71-7.25 (8H, m), 5.02 (1H, d), 3.61 (1H, d), 3.16 (2H, m), 2.77-2.52 (7H, m), 2.24 (1H, dd), 2.01 (1H, dd), 1.31 (1H, m); High-resolution mass spectroscopy (HRMS), $C_{23}H_{26}N_3O_2S_2$ $[M+H]^+$, 440.1461 calculated, 440.1466 detected.

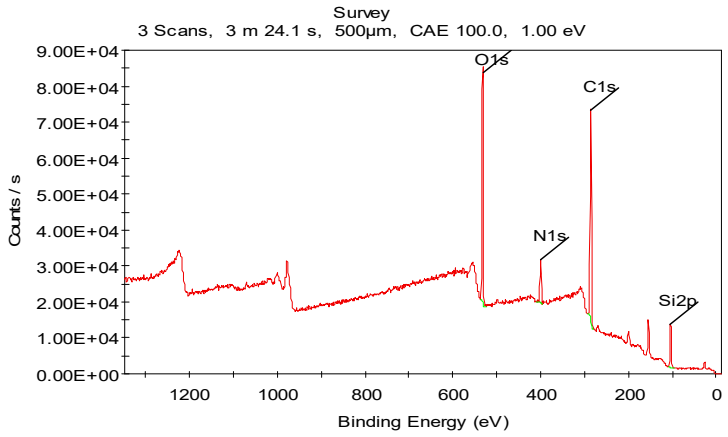

O	22.48
C	58.57
N	7.53
Si	11.43
S	0

312

313 **CF-DBCO**

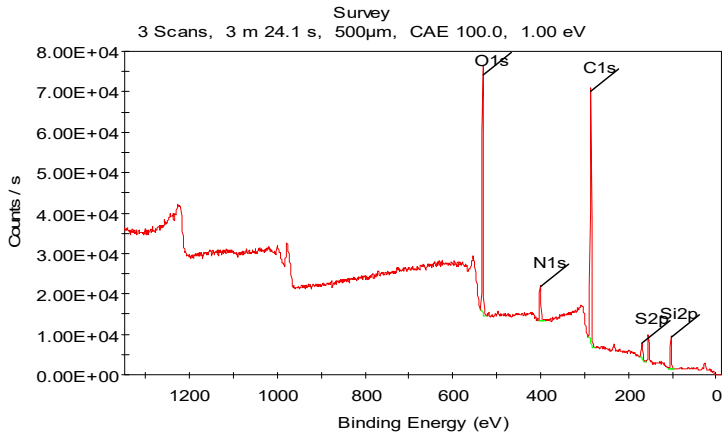

O	22.8
C	62.38
N	6.02
Si	6.73
S	2.07

314

315 **CF-NP-DBCO**

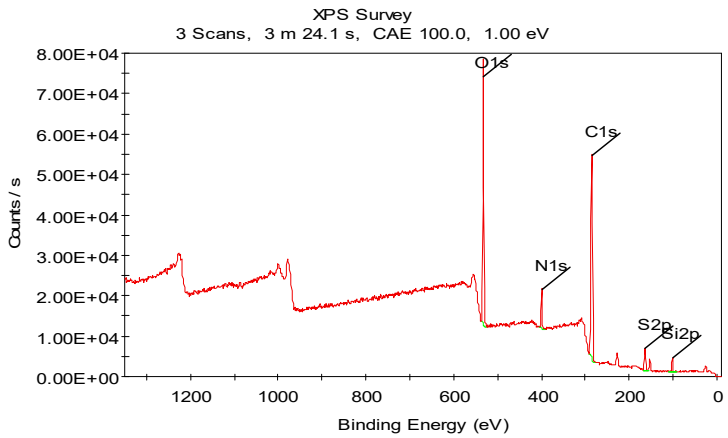

O	25.76
C	62.37
N	5.83
S	2.69
Si	3.35

316

317 **CF-NP-SS-DBCO**

Supplementary Figure 6. XPS analysis of different bio-orthogonal films.

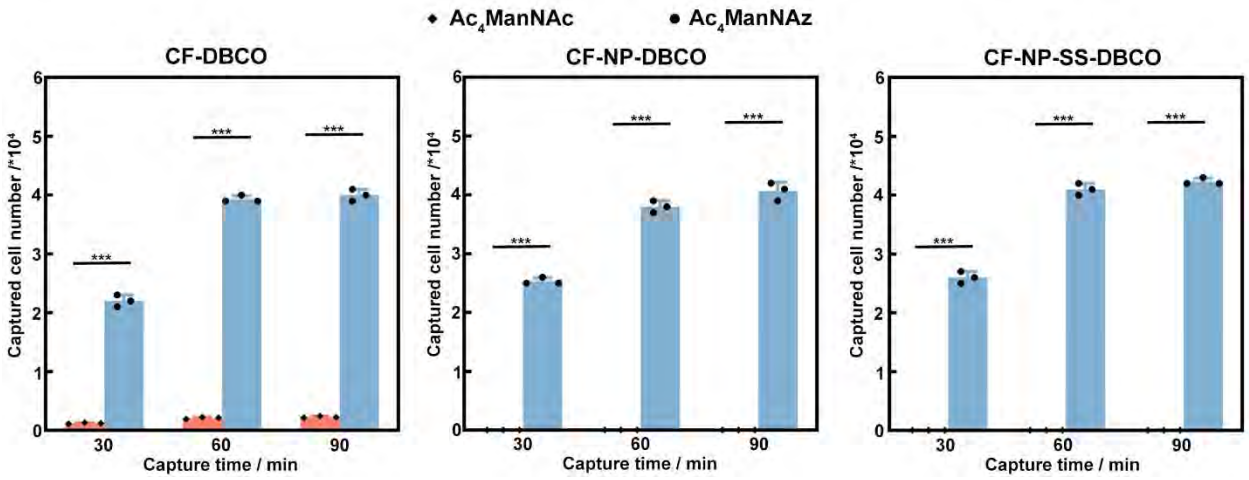

Supplementary Figure 7. Capture time-captured cell number (from a total of 50000 cells) of MGE-treated H524 cells with/without azido groups (*** denotes $p < 0.001$).

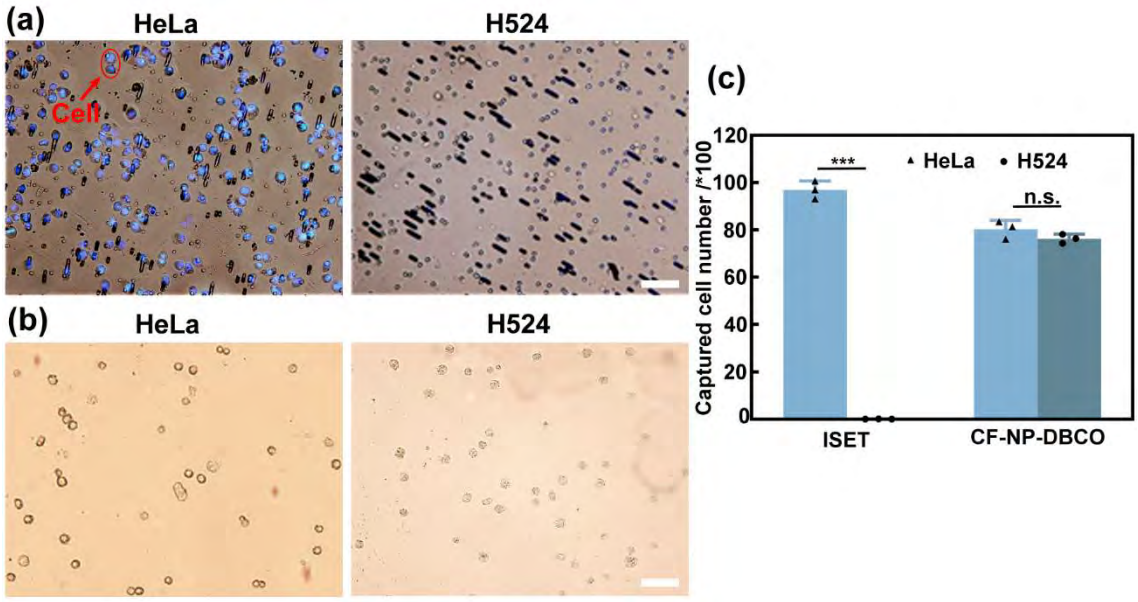

Supplementary Figure 8. Comparison of capturing capability between the bio-orthogonal films and commercial ISET. (a) HeLa cells (left) and H524 cells (right) captured by ISET standard membrane (scale bar = 50 μm); (b) HeLa cells (left) and H524 cells (right) captured by bio-orthogonal films (scale bar = 50 μm); (c) Statistical analysis (*** denotes $p < 0.001$).

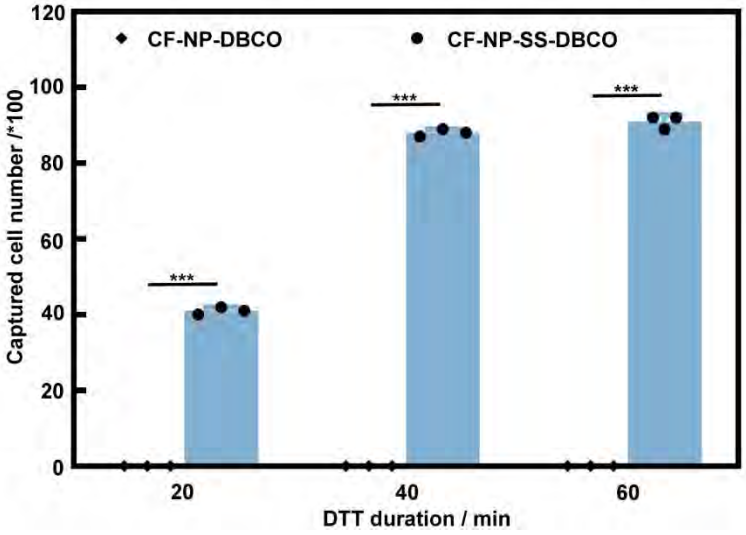

Supplementary Figure 9. DTT treatment duration-H524 cells release efficiency of CF-NP-DBCO and CF-NP-SS-DBCO (*** denotes $p < 0.001$).

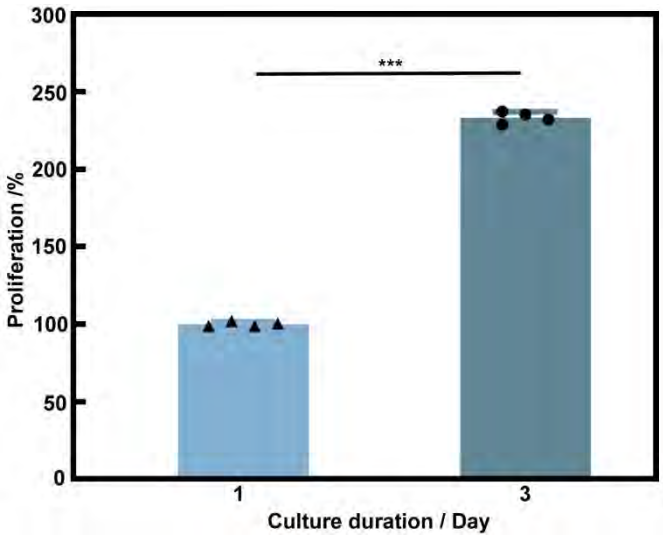

Supplementary Figure 10. Long-term viability of H524 cells by normal cultivation (*** denotes $p < 0.001$).

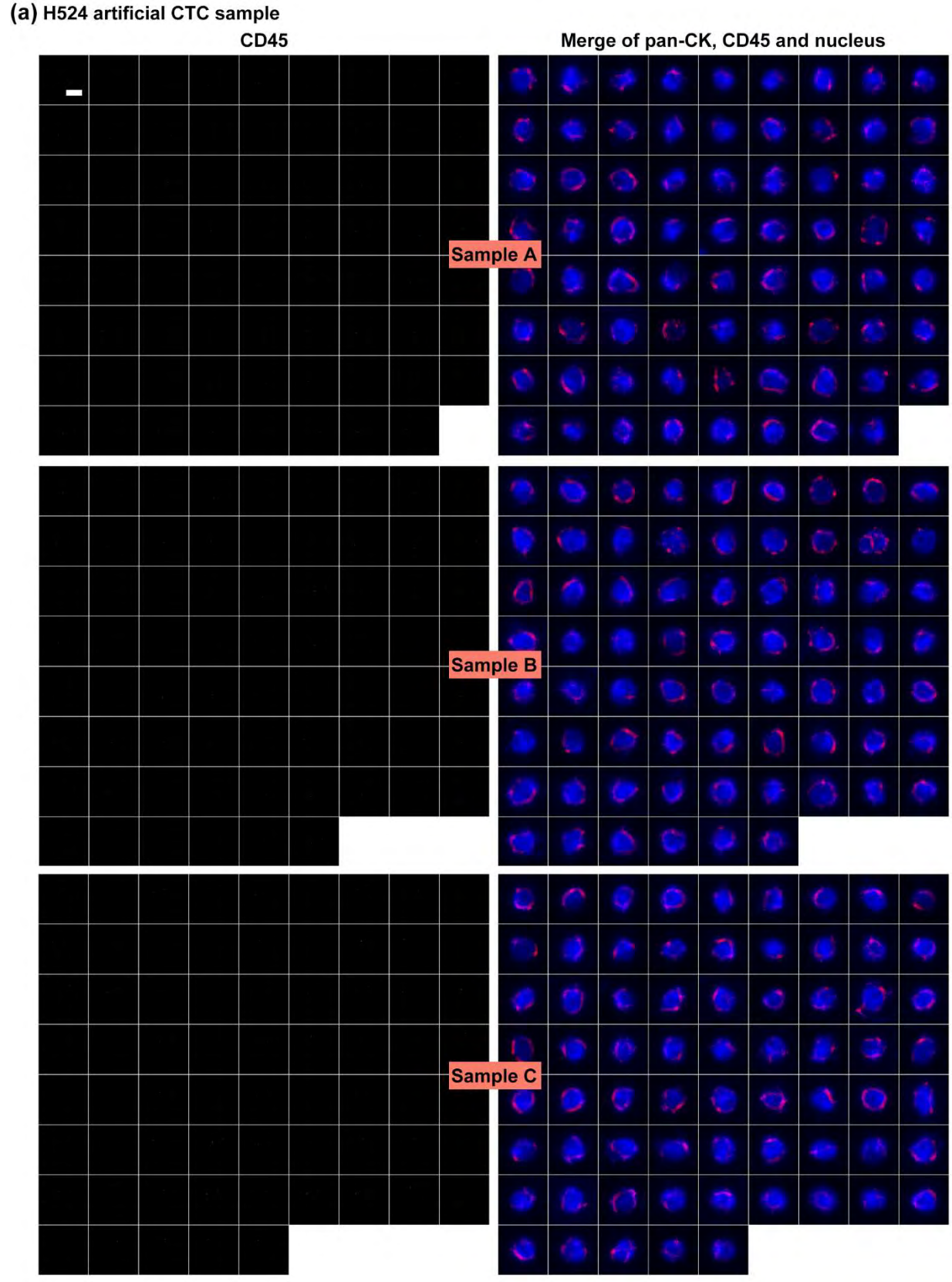
(a) H524 artificial CTC sample
CD45
Merge of pan-CK, CD45 and nucleus
Sample A
Sample B
Sample C

371

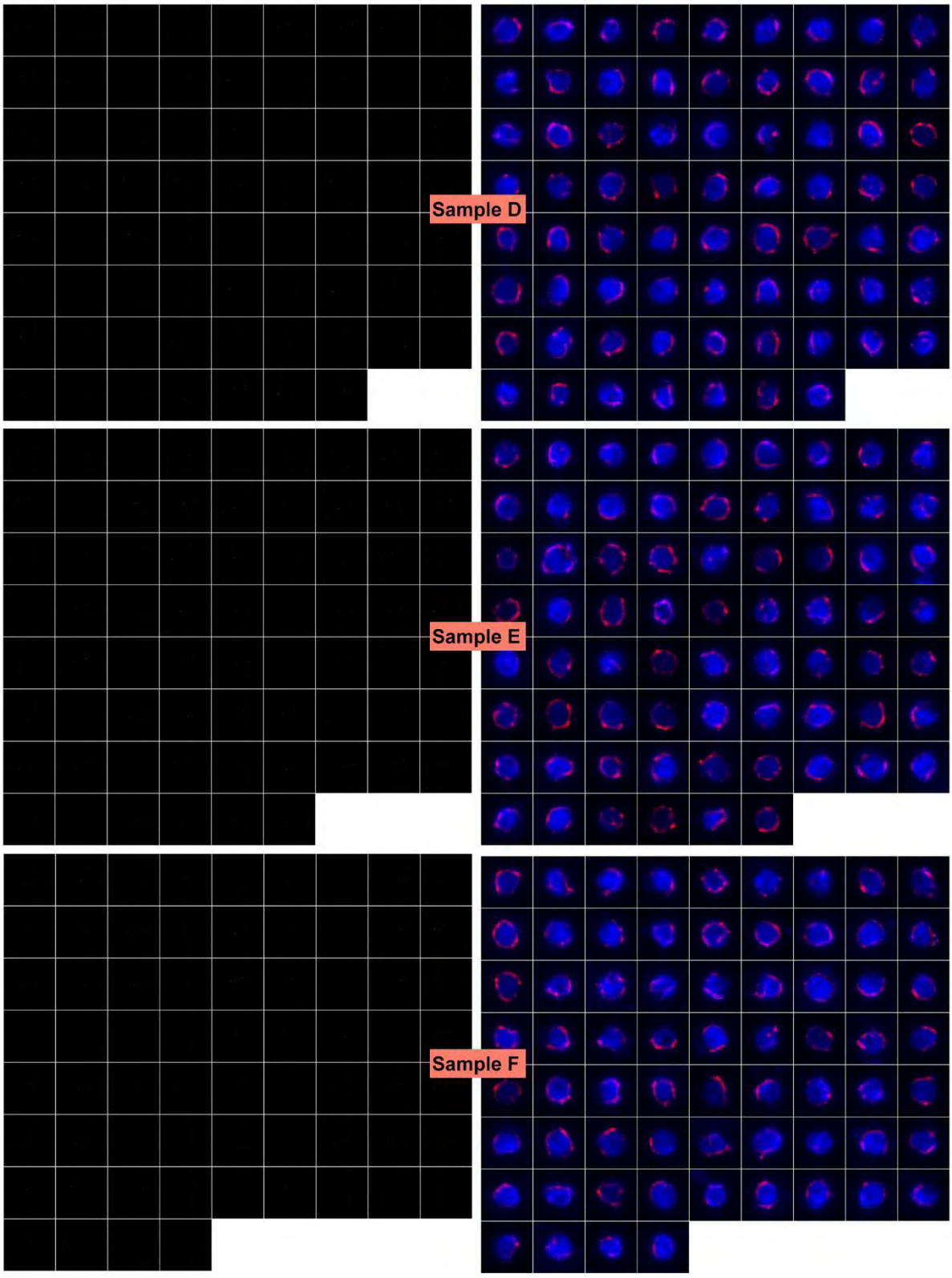

372

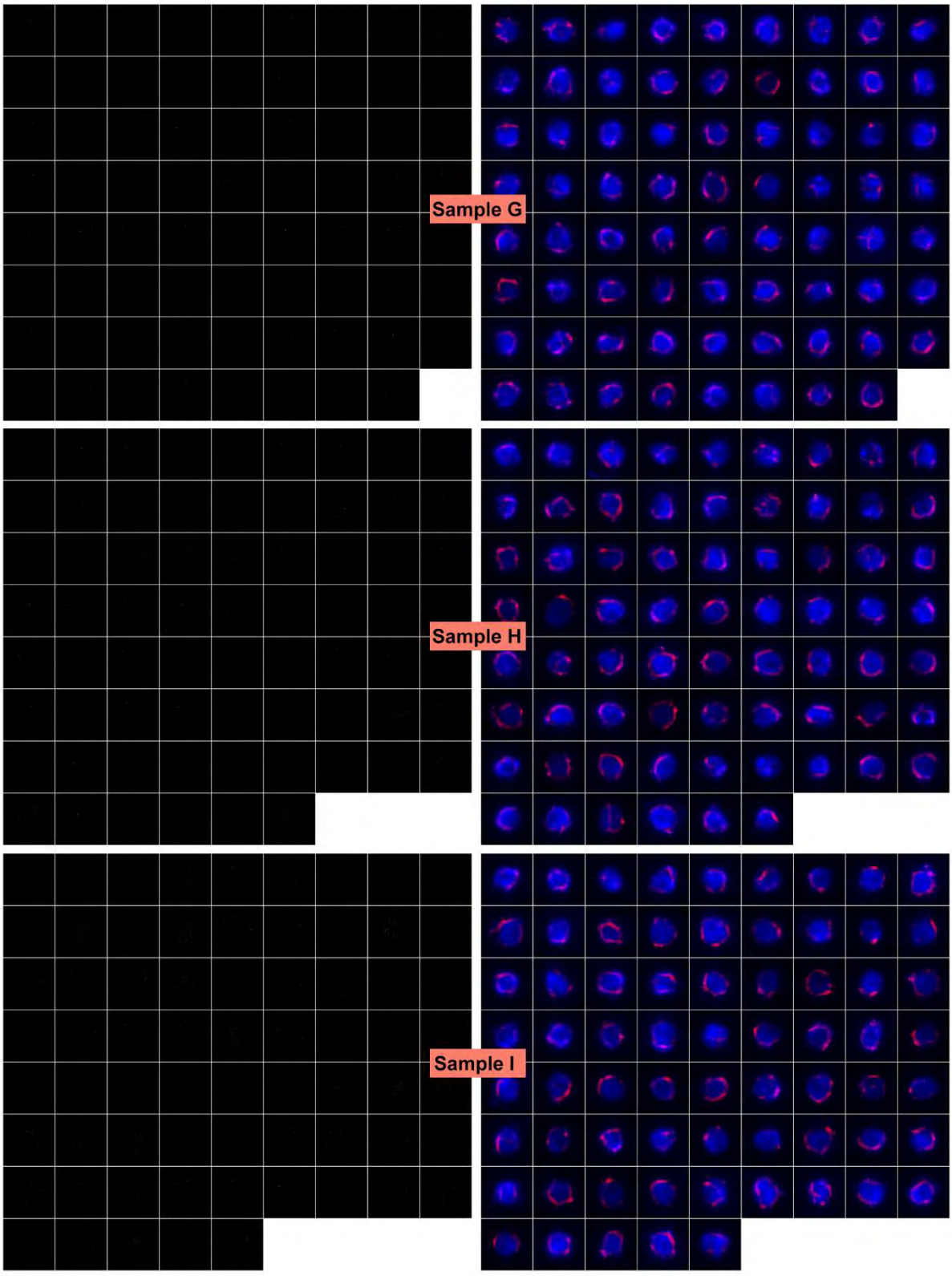

373

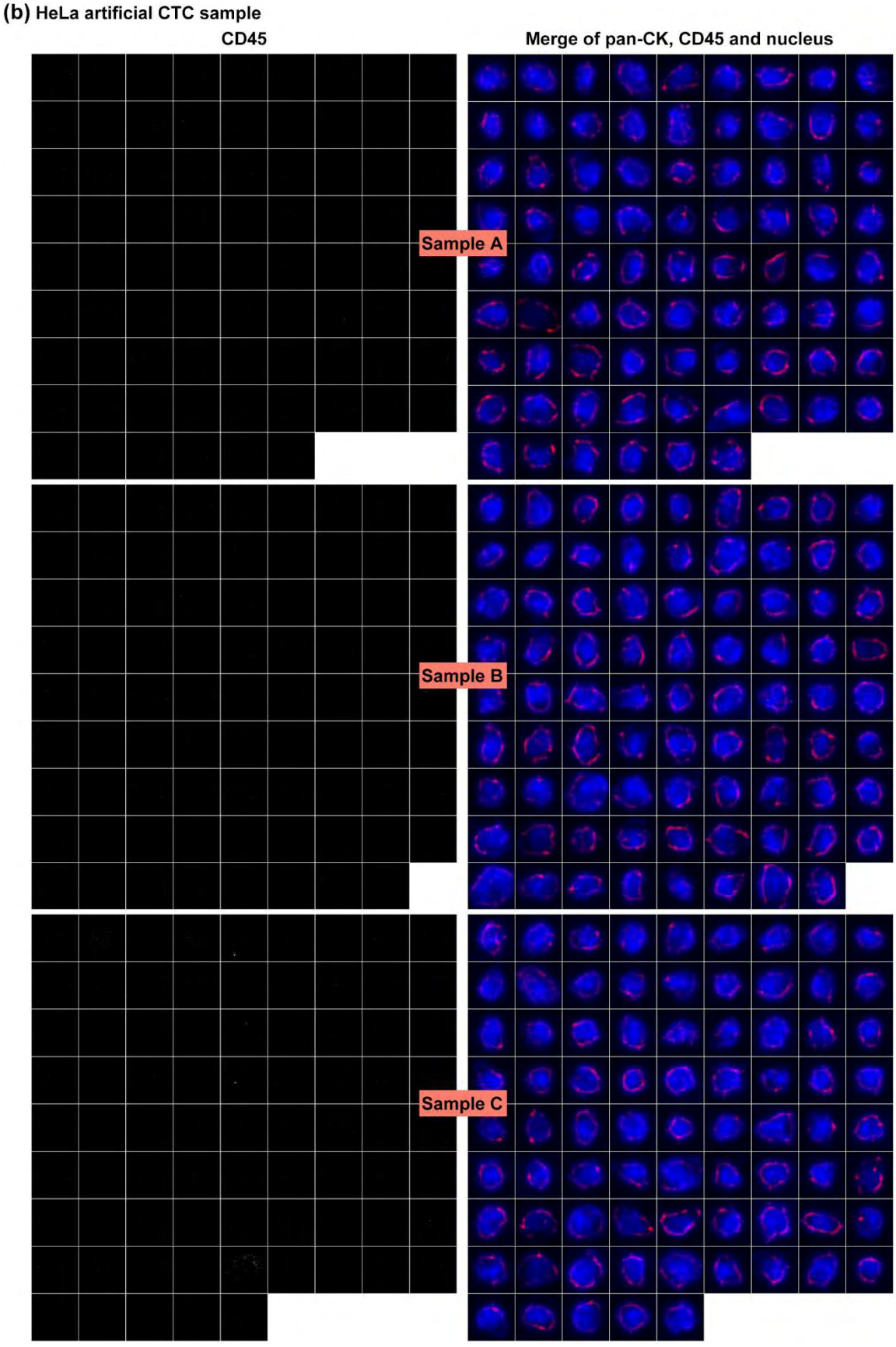
(b) HeLa artificial CTC sample
CD45
Merge of pan-CK, CD45 and nucleus
Sample A
Sample B
Sample C

374

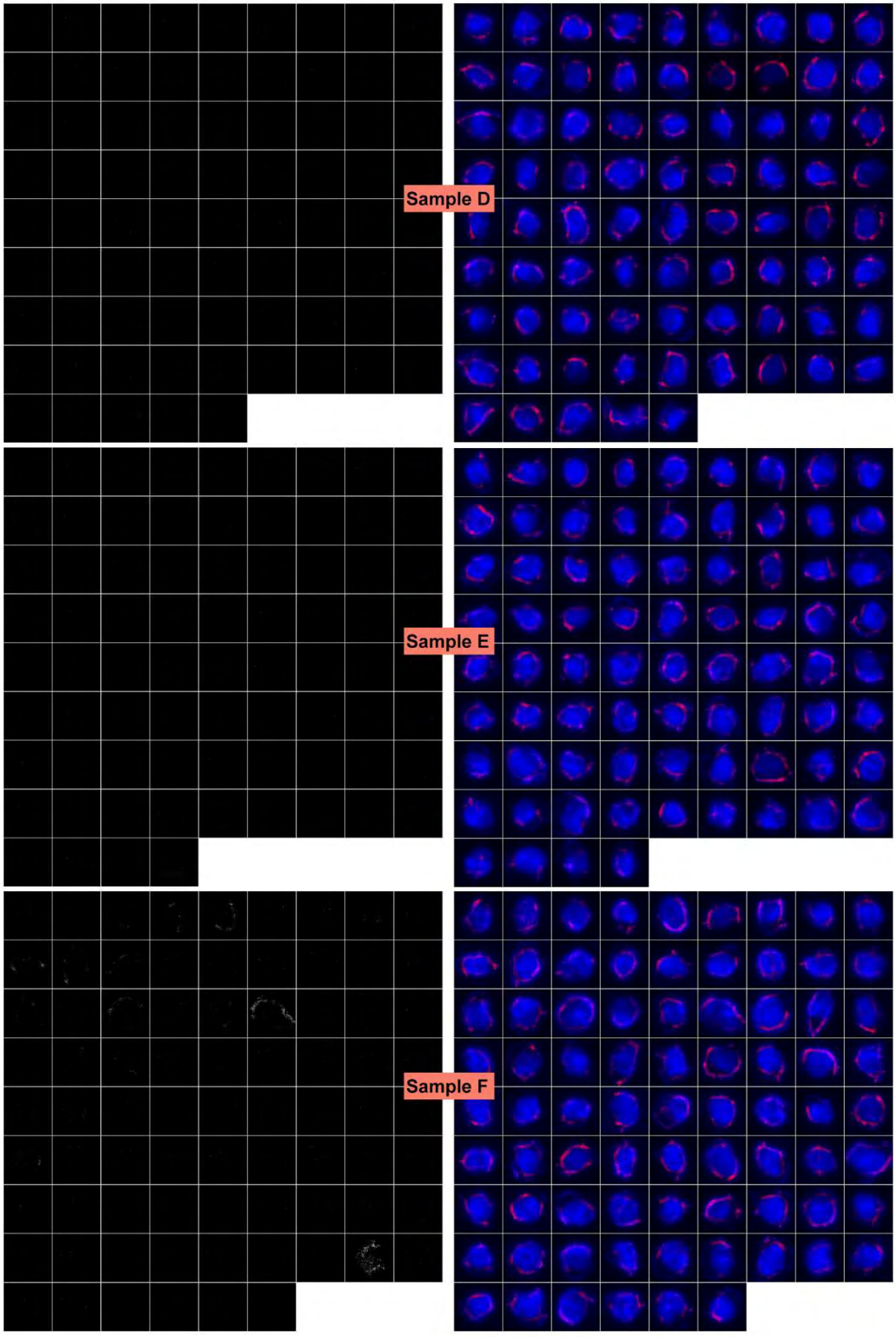

375

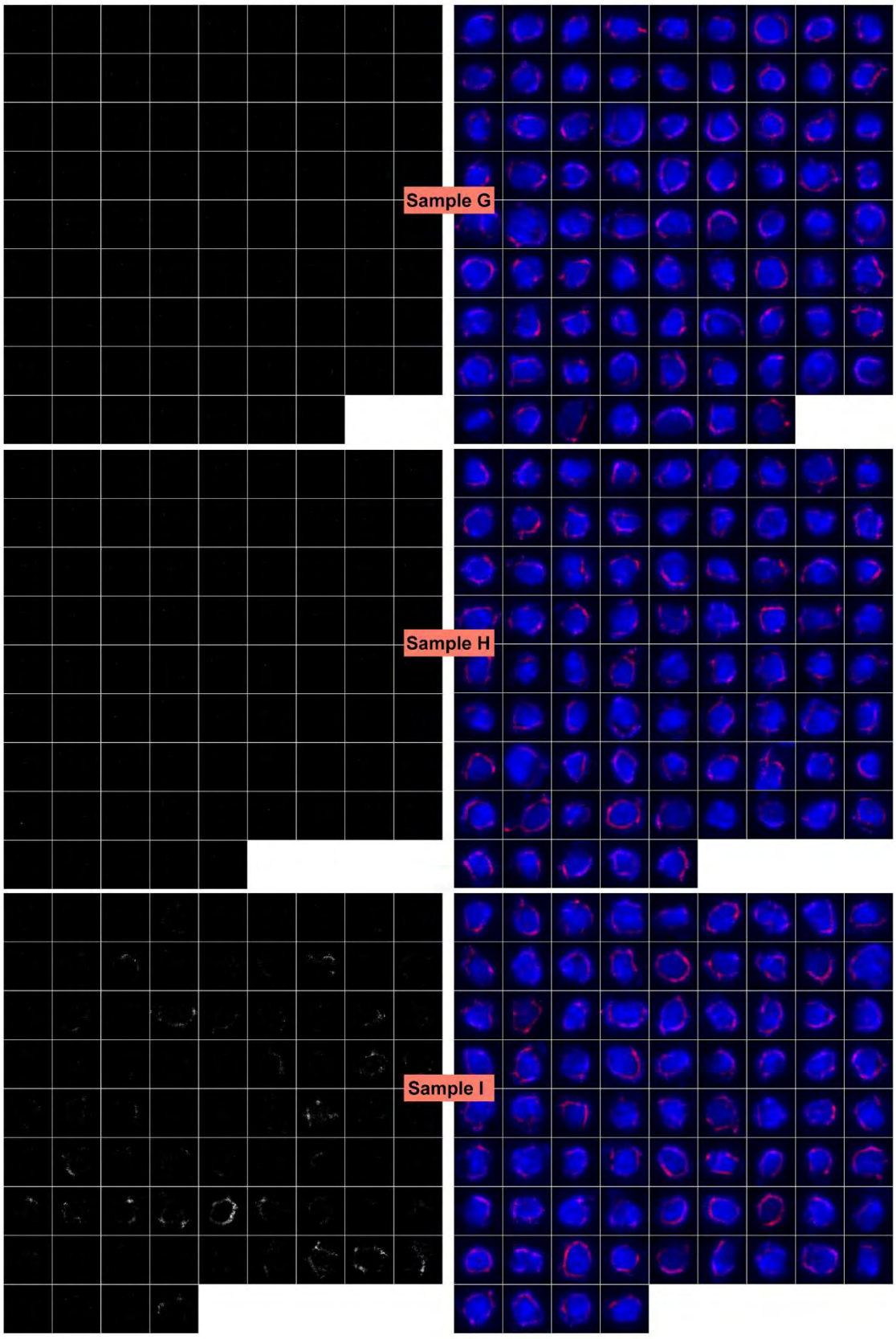

376

Supplementary Figure 11. Fluorescent pictures of artificial CTCs (100 cancer cells spiked in 1 mL of blood samples) captured by the bio-orthogonal films and identified by the nuclei (blue), CD45 (white), and pan-CK (red) staining (scale bar = 5 μm). (a) Captured H524 cells in blood samples and (b) Captured HeLa cells in blood samples.

Patient information: male, 73 years old, liver cancer.

(a) Picture by 590 nm and 490 nm excitation luminescence

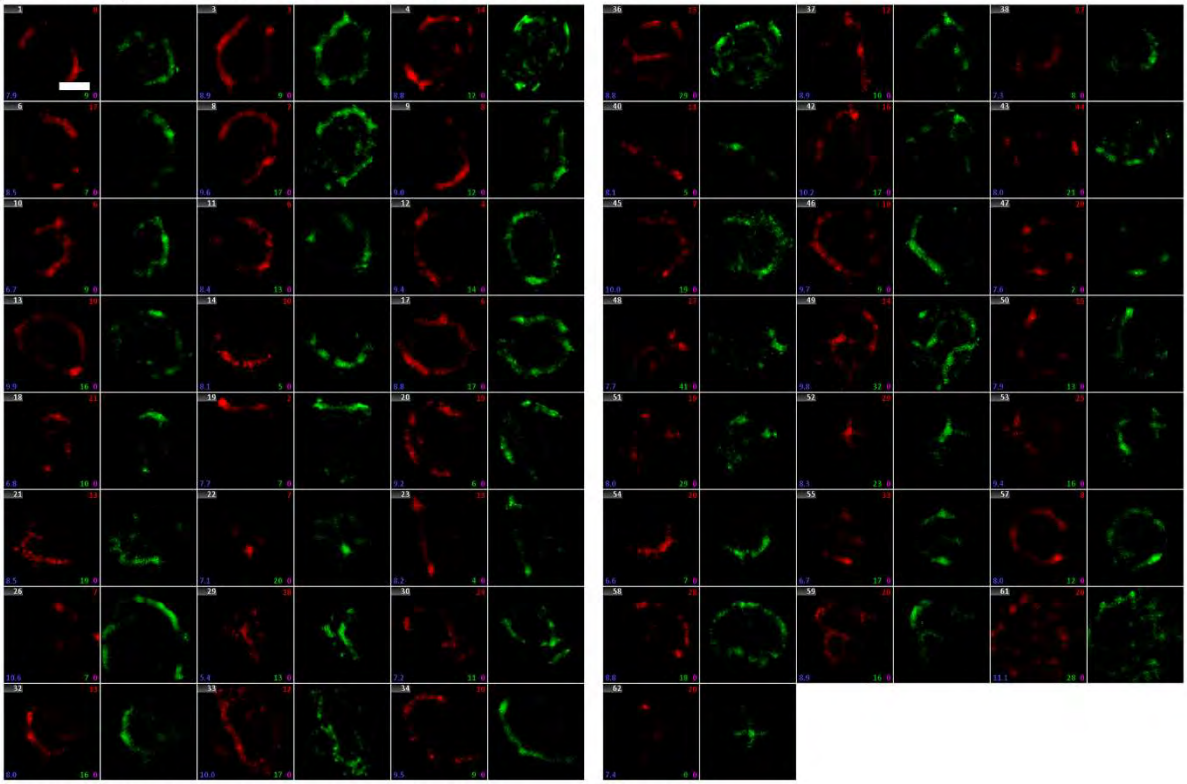

(b) Picture by 750nm excitation luminescence

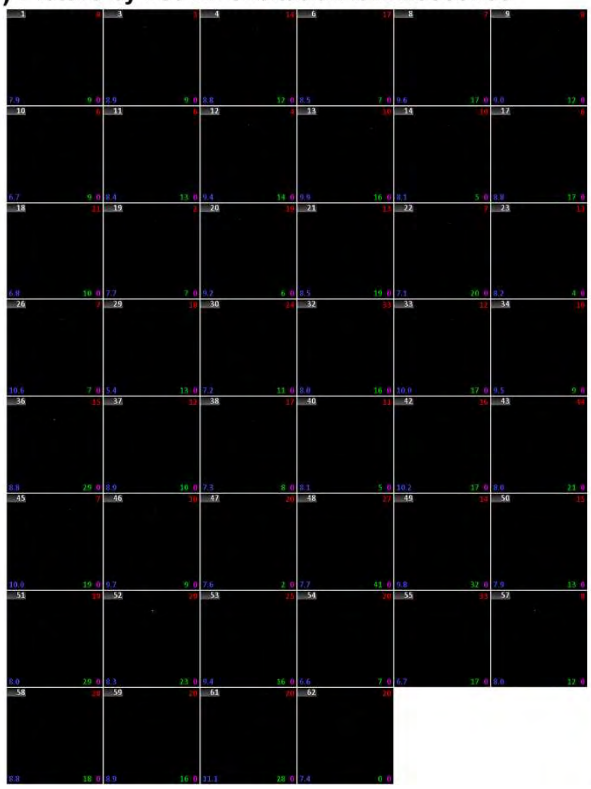

(c) Merge

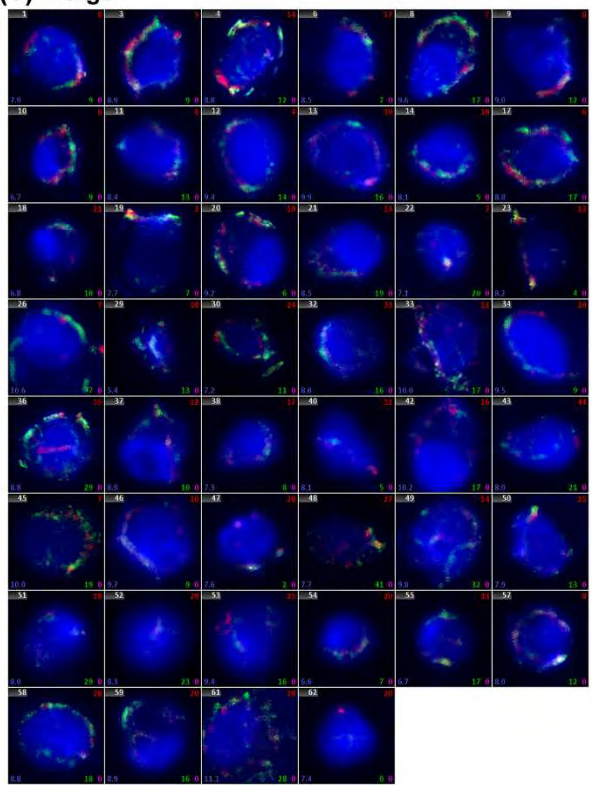

400

Supplementary Figure 12. Fluorescent pictures of ISET-separated clinical CTCs modified by MGE with pan-CK as the positive CTCs biomarker (scale bar = 5 μm). (a) Red referring to pan-CK and green color representing the azido group; (b) White color refers to CD45; (c) Merged images of pan-CK, azido group, CD45, and nuclei.

Patient information: Sample A, male, 52 years old, liver cancer;
Sample B, Female, 61 years old, lung cancer;
Sample C, Male, 45 years old, nasopharyngeal cancer.

(a) Picture by 590 nm and 490 nm excitation luminescence

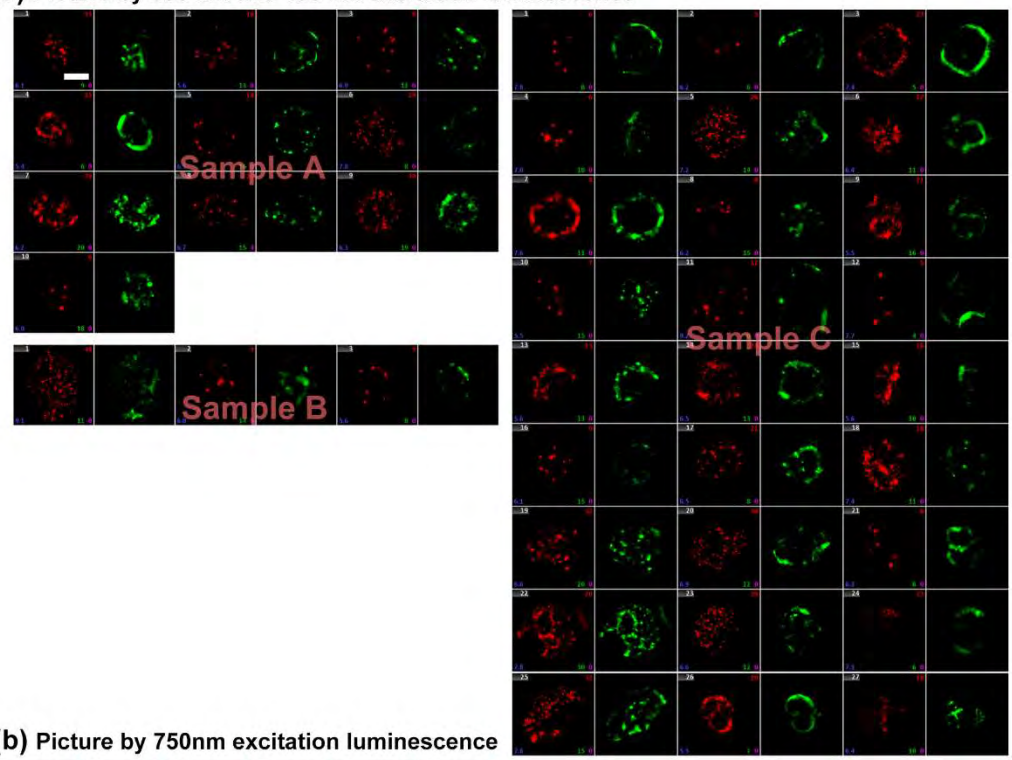

(b) Picture by 750nm excitation luminescence

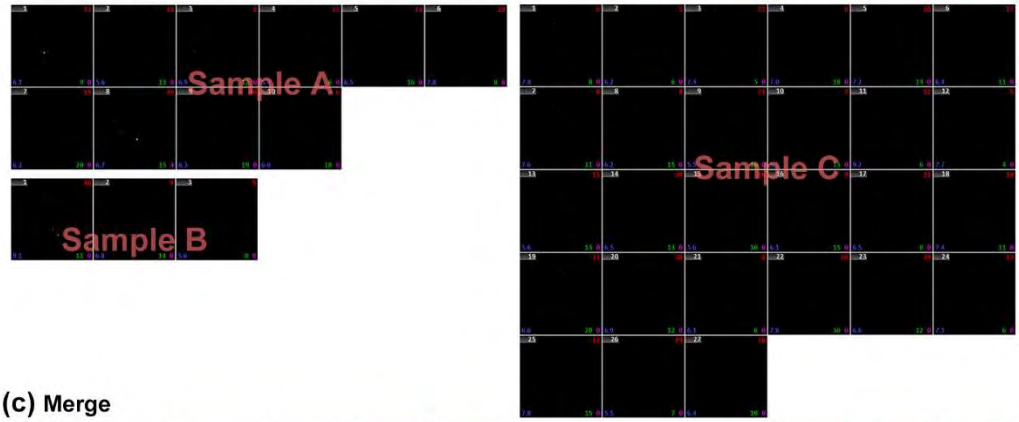

(c) Merge

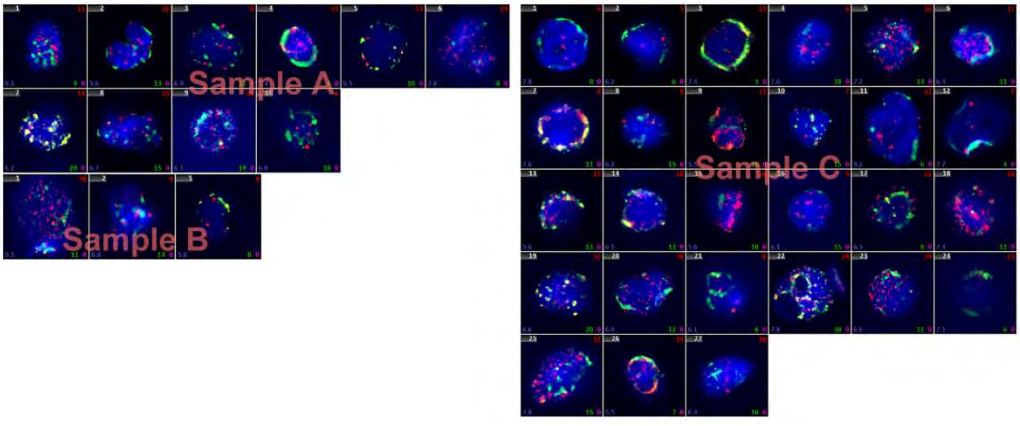

406

Supplementary Figure 13. Fluorescent pictures or ISET-separated clinical CTCs modified by MGE with EpCAM-CKs as the positive CTCs biomarker (scale bar = 5 μm). (a) Red referring to EpCAM-CKs and green referring to the azido group; (b) White color refers to CD45; (c) Merged images of EpCAM-CKs, azido group, CD45 and nuclei.

P1

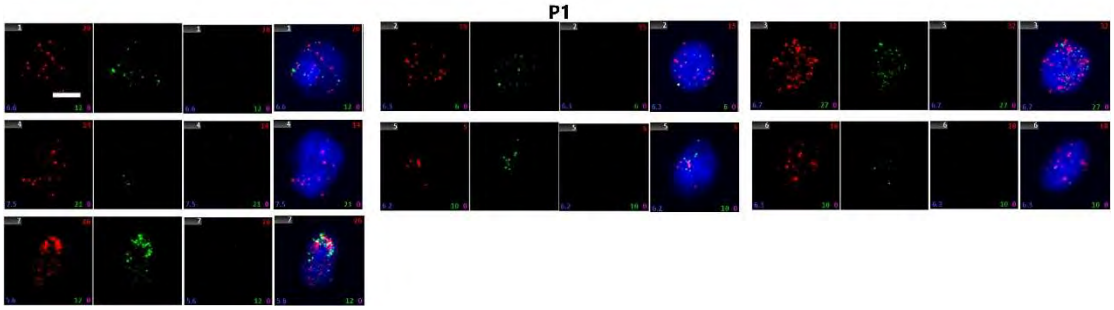

P2

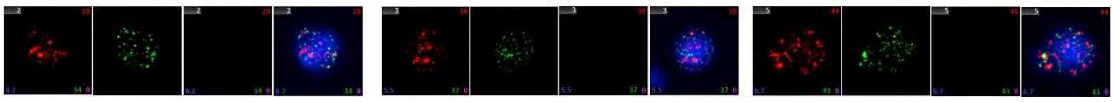

P3

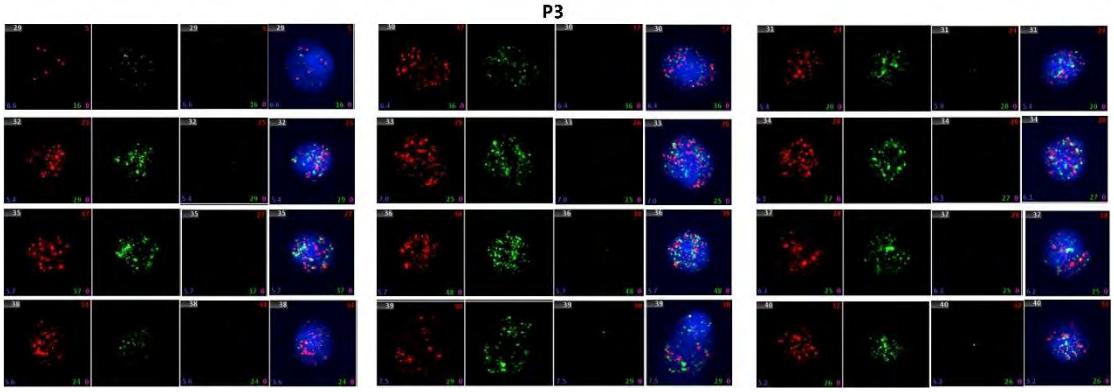

P4

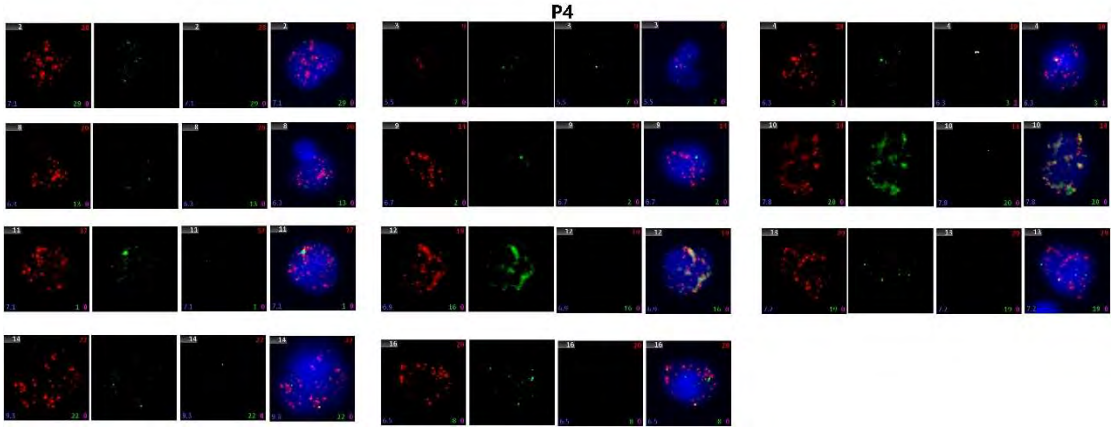

P5

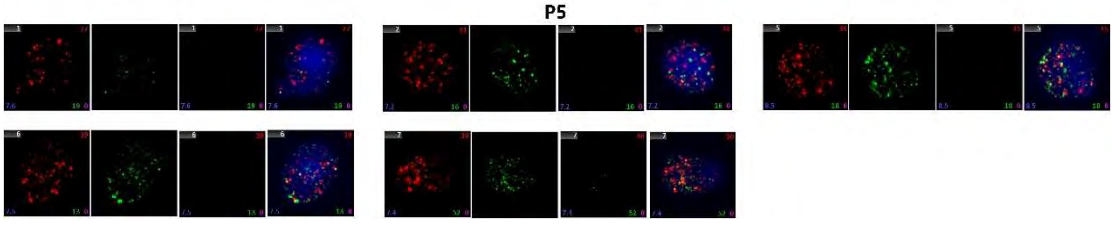

433

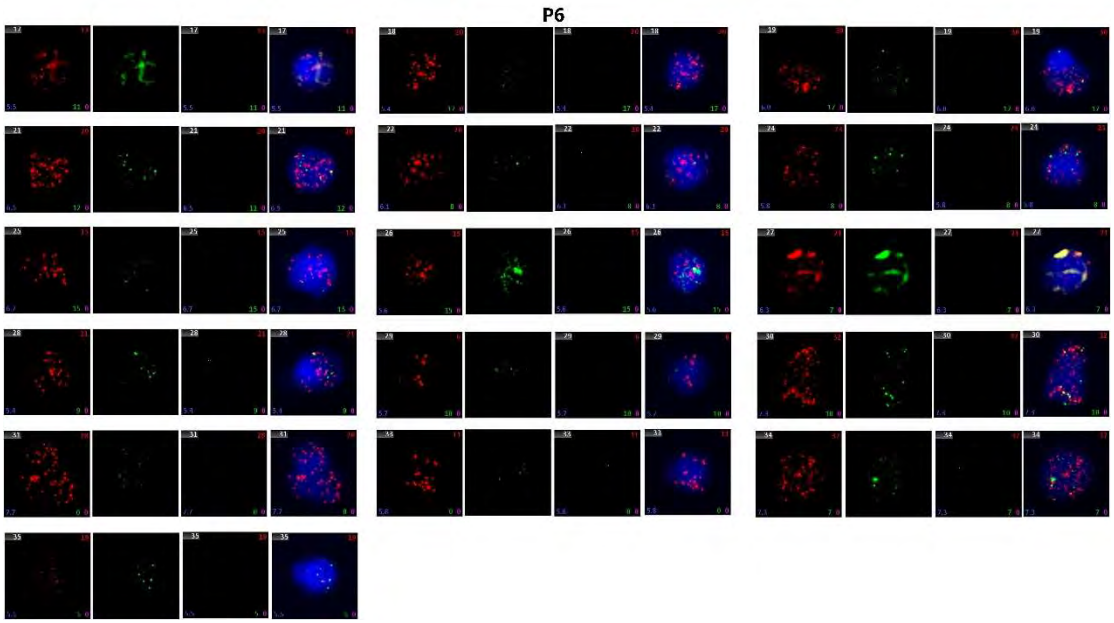

434

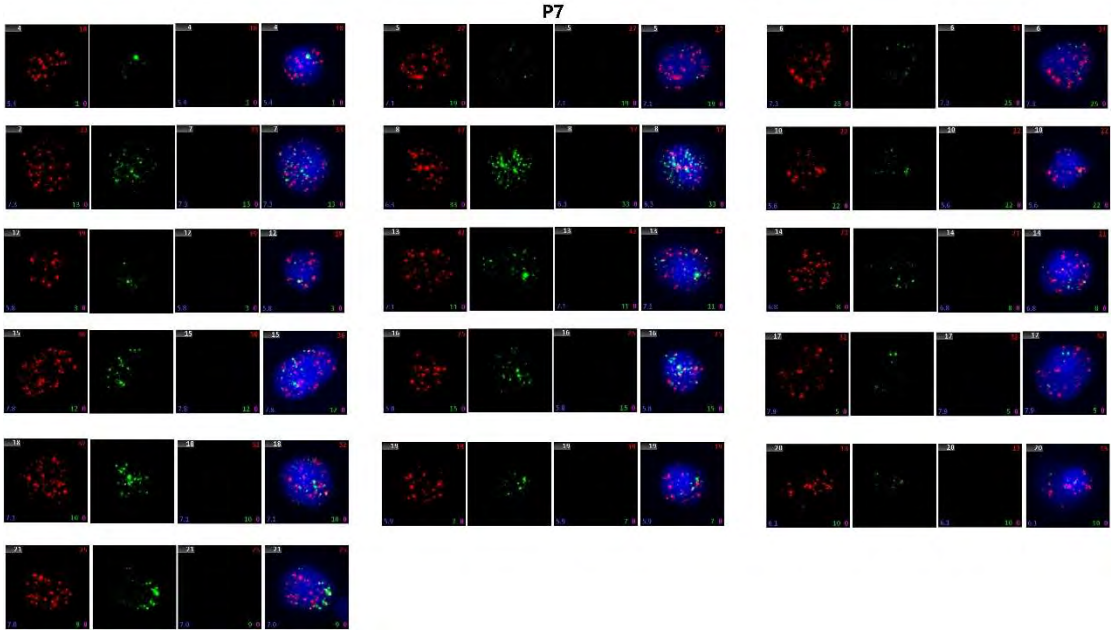

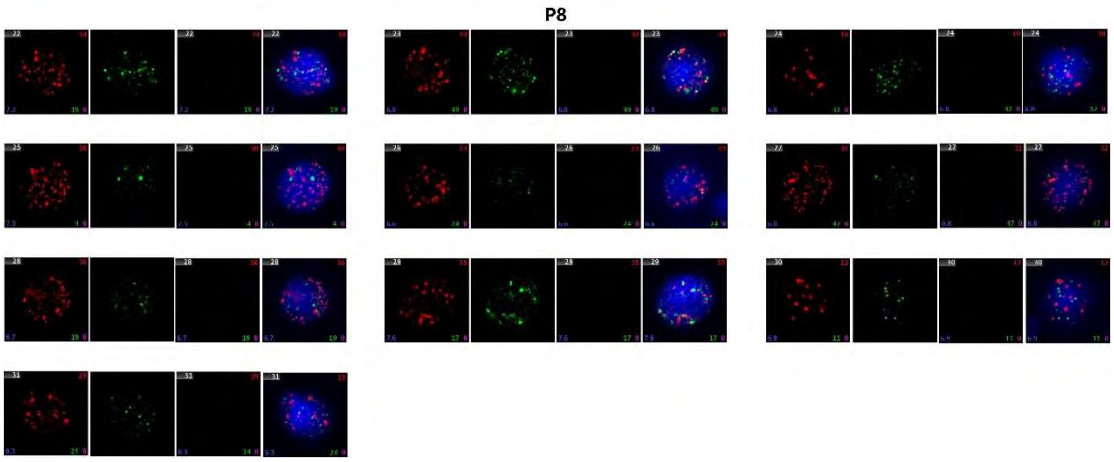

435

436 **Supplementary Figure 14**. Fluorescent pictures of the clinical CTCs captured by bio-orthogonal

437 films and identified by the nucleus (blue), CD45 (white), EpCAM (red), and vimentin (green)

438 staining (scale bar = 5 μm).

439

440

441

442

443

444

445

446

447

448

449

450

451

452

P9

Bio-orthogonal film

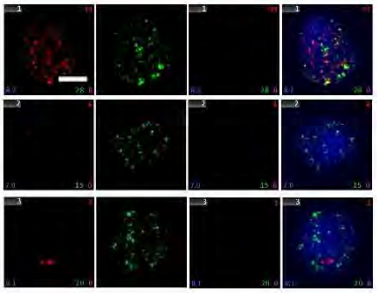

中科纳泰 nanopep | 肿瘤猎手 TUMORFISHER TumorFisher®

外周血循环肿瘤细胞(CTC)检测结果报告

样本编号：SIAT202301　　送检日期：2023年8月16日

送检单位：暨南大学第二临床医学院

CTC检测结果

血液样本中富集和检测到符合 CTC 特征的细胞数：0 个。

1 荧光显微图像

（1）CTC：

合成图	明 场	DAPI	CD45	CK	CD45+DAPI	CK+DAPI

CTC图片从检测指标中获取，最多展示2组照片。

（2）WBC：

合成图	明 场	DAPI	CD45	CK	CD45+DAPI	CK+DAPI

检测时间：2023年8月16日

453

P10

Bio-orthogonal film

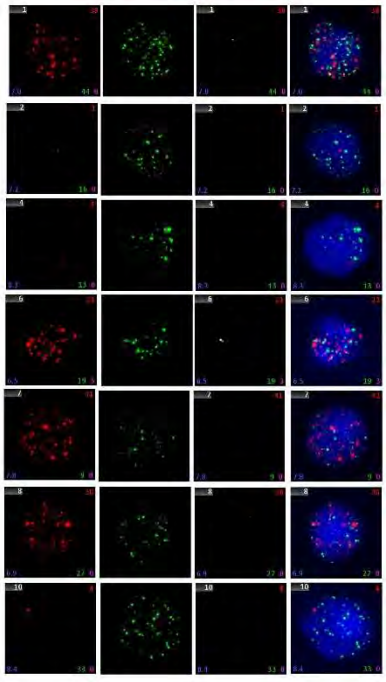

中科纳泰 nanopep | 肿瘤猎手 TUMORFISHER TumorFisher®

外周血循环肿瘤细胞(CTC)检测结果报告

样本编号：SIAT202302　　送检日期：2023年8月24日

送检单位：暨南大学第二临床医学院

CTC检测结果

血液样本中富集和检测到符合 CTC 特征的细胞数：2 个。

1 荧光显微图像

（1）CTC：

合成图	明 场	DAPI	CD45	CK	CD45+DAPI	CK+DAPI

CTC图片从检测指标中获取，最多展示2组照片。

（2）WBC：

合成图	明 场	DAPI	CD45	CK	CD45+DAPI	CK+DAPI

检测时间：2023年8月24日

454

P11

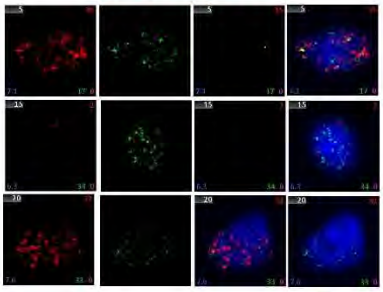

中科纳泰 nanopep | 肿瘤猎手 TUMORFISHER TumorFisher®

外周血循环肿瘤细胞(CTC)检测结果报告

样本编号：SIAT202303　　送检日期：2023年9月4日

送检单位：暨南大学第二临床医学院

CTC检测结果

血液样本中富集和检测到符合 CTC 特征的细胞数：1 个。

1 荧光显微图像

（1）CTC：

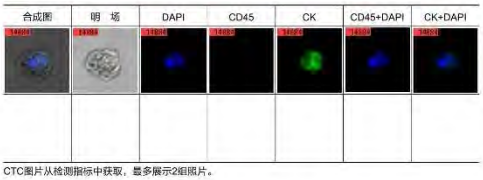

CTC图片从检测指标中获取，最多展示2组照片。

（2）WBC：

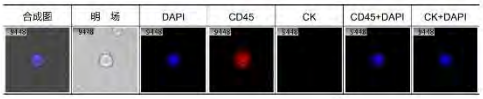

检测时间：2023年9月4日

455

P12

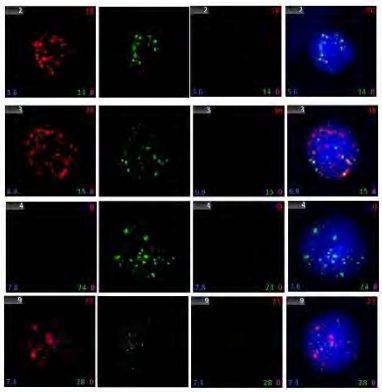

中科纳泰 nanopep | 肿瘤猎手 TUMORFISHER TumorFisher®

外周血循环肿瘤细胞(CTC)检测结果报告

样本编号：SIAT202304　　送检日期：2023年9月13日

送检单位：暨南大学第二临床医学院

CTC检测结果

血液样本中富集和检测到符合 CTC 特征的细胞数：3 个。

1 荧光显微图像

（1）CTC：

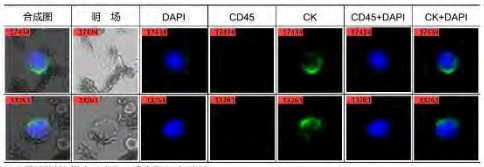

CTC图片从检测指标中获取，最多展示2组照片。

（2）WBC：

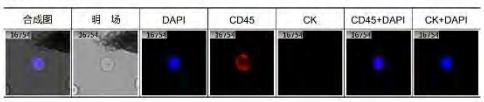

检测时间：2023年9月13日

456

P13

Bio-orthogonal film

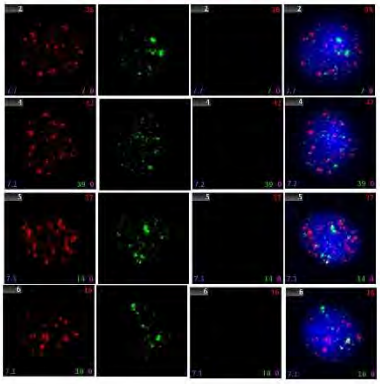

中科纳泰 | 肿瘤博宇 TumorFisher®

外周血循环肿瘤细胞(CTC)检测结果报告

样本编号：SIAT202305　　送检日期：2023年9月23日

送检单位：暨南大学第二临床医学院

CTC检测结果

血液样本中富集和检测到符合 CTC 特征的细胞数：2 个。

1 荧光显微图像

（1）CTC：

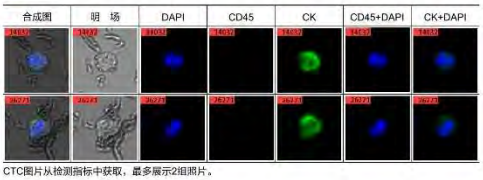

CTC图片从检测指标中获取，最多展示2组照片。

（2）WBC：

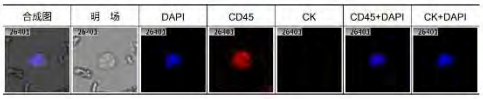

检测时间：2023年9月23日

457

P14

Bio-orthogonal film

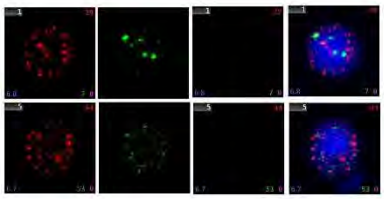

中科纳泰 | 肿瘤博宇 TumorFisher®

外周血循环肿瘤细胞(CTC)检测结果报告

样本编号：SIAT202306　　送检日期：2023年9月23日

送检单位：暨南大学第二临床医学院

CTC检测结果

血液样本中富集和检测到符合 CTC 特征的细胞数：2 个。

1 荧光显微图像

（1）CTC：

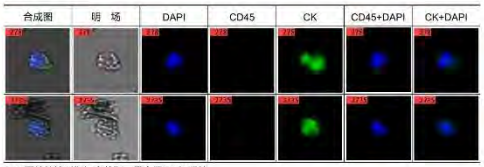

CTC图片从检测指标中获取，最多展示2组照片。

（2）WBC：

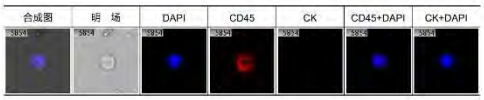

检测时间：2023年9月23日

458

P15

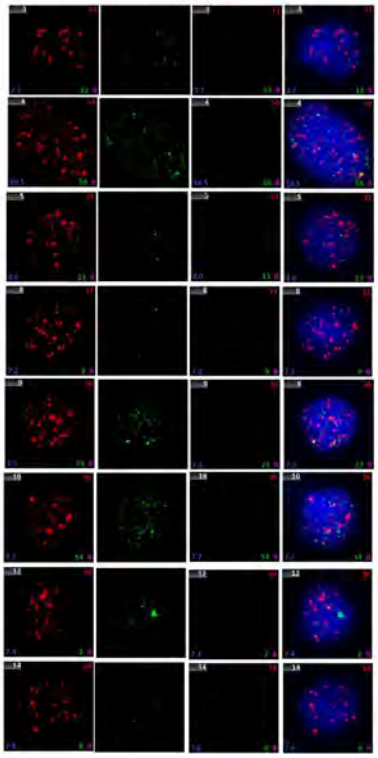

TumorFisher®

外周血循环肿瘤细胞(CTC)检测结果报告

样本编号：SIAT202308　　送检日期：2023年9月23日

送检单位：暨南大学第二临床医学院

CTC检测结果

2mL 血液样本中富集和检测到符合 CTC 特征的细胞数：7 个。

1 荧光显微图像

（1）CTC：

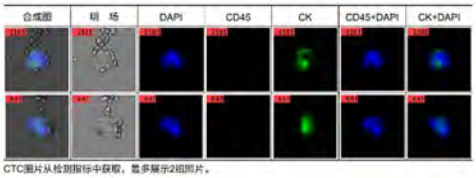

CTC图片从检测指标中获取，最多展示2组照片。

（2）WBC：

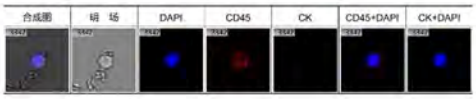

检测时间：2023年9月23日　　检测员：薛建

459

P16

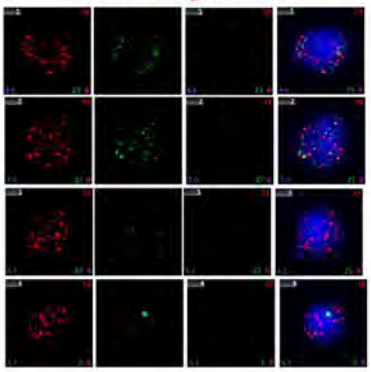

TumorFisher®

外周血循环肿瘤细胞(CTC)检测结果报告

样本编号：SIAT202309　　送检日期：2023年9月27日

送检单位：暨南大学第二临床医学院

CTC检测结果

2mL 血液样本中富集和检测到符合 CTC 特征的细胞数：1 个。

1 荧光显微图像

（1）CTC：

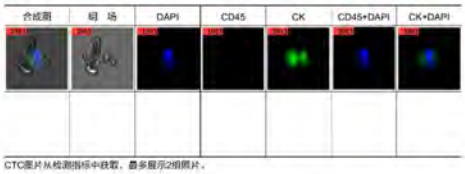

CTC图片从检测指标中获取，最多展示2组照片。

（2）WBC：

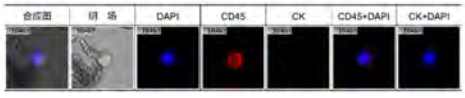

检测时间：2023年9月27日　　检测员：薛建

460

P17

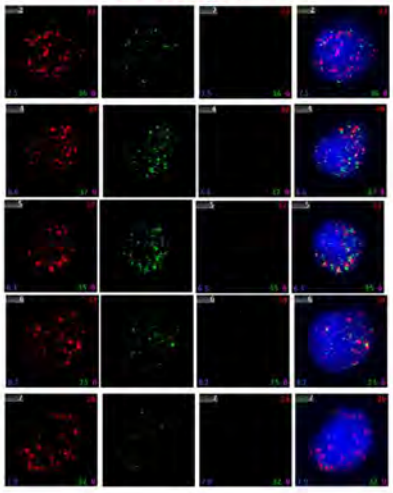

TumorFisher®

外周血循环肿瘤细胞(CTC)检测结果报告

样本编号：SIAT202310　　送检日期：2023年9月27日

送检单位：暨南大学第二临床医学院

CTC检测结果

2mL 血液样本中富集和检测到符合 CTC 特征的细胞数：1 个。

1 荧光显微图像

（1）CTC：

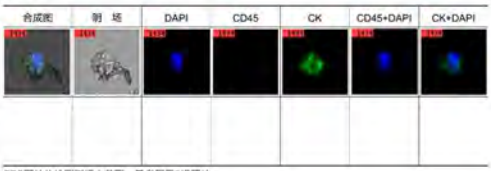

CTC图片从检测指标中获取，最多展示2组照片。

（2）WBC：

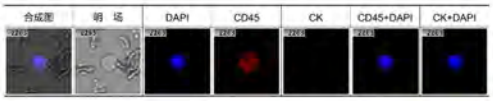

检测时间：2023年9月27日　　检测员：薛建

461

P18

TumorFisher®

外周血循环肿瘤细胞(CTC)检测结果报告

样本编号：SIAT202311　　送检日期：2023年9月27日

送检单位：暨南大学第二临床医学院

CTC检测结果

2mL 血液样本中富集和检测到符合 CTC 特征的细胞数：2 个。

1 荧光显微图像

（1）CTC：

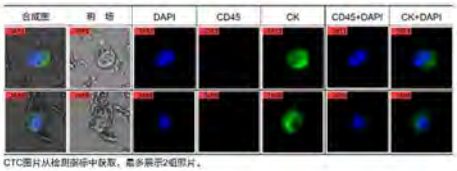

CTC图片从检测指标中获取，最多展示2组照片。

（2）WBC：

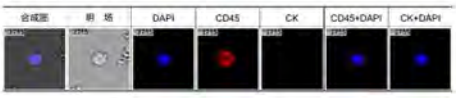

检测时间：2023年9月27日　　检测员：薛建

462

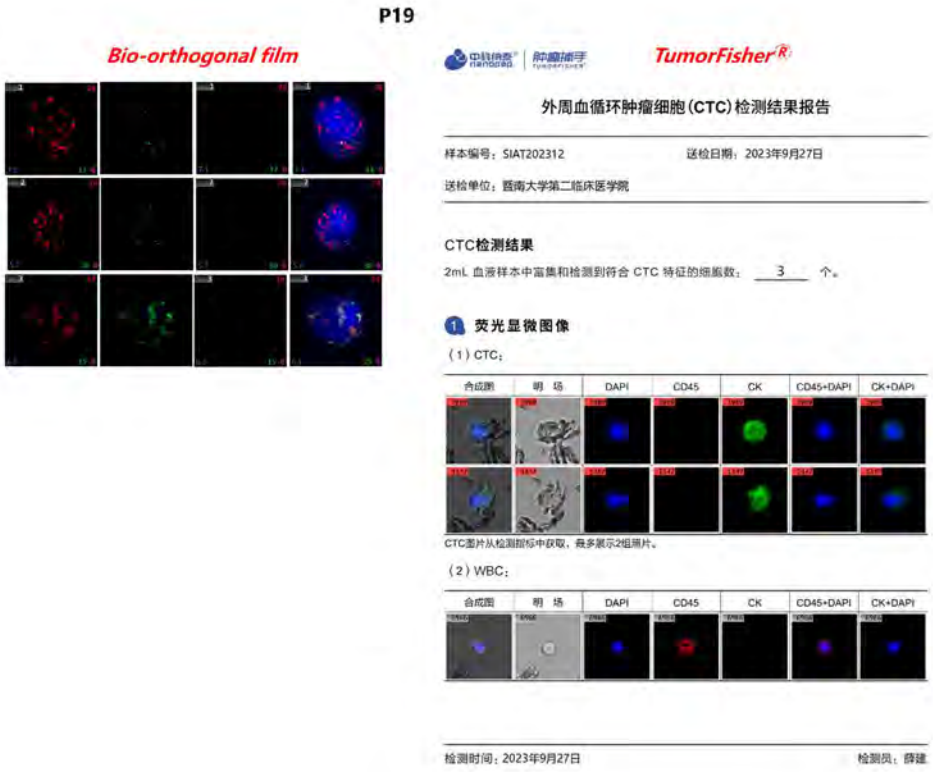

463

464 **Supplementary Figure 15**. Direct comparison between the bio-orthogonal films and
465 TumorFisher® system about clinical CTCs detection. The CTCs captured by bio-orthogonal films
466 are identified by the nucleus (blue), CD45 (white), EpCAM (red), and vimentin (green) staining,
467 while the CTCs captured by TumorFisher® are identified by the nucleus (blue), CD45 (red) and
468 CK (green) staining.

469

470

471

472

473

474

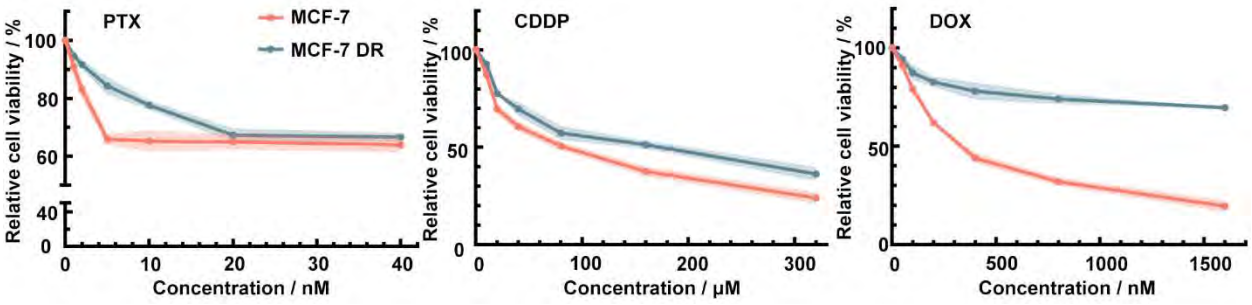

475

476 **Supplementary Figure 16**. Drug concentration-relative cell viability of MCF-7 cells and MCF-7

477 DR cells determined by the CCK-8 assay.

478

479

480

481

482

483

484

485

486

487

488

489

490

491

492

493

494

Supplementary Table 1. Information of donors.

No.	Cancer Type	Gender	Age
H1	healthy	M	36
H2	healthy	F	67
H3	healthy	M	34
H4	healthy	F	32
P1	breast cancer	F	67
P2	liver cancer	M	62
P3	liver cancer	M	57
P4	breast cancer	F	59
P5	gastric cancer	F	65
P6	nasopharyngeal carcinoma	M	57
P7	lung cancer	M	54
P8	liver cancer	F	49
P9	colon cancer	M	28
P10	rectal cancer	M	59
P11	rectal cancer	M	70
P12	osteosarcoma	M	14
P13	cervical cancer	F	37
P14	cervical cancer	F	64
P15	rectal cancer	M	68
P16	nasopharyngeal carcinoma	M	22

P17	nasopharyngeal carcinoma	M	56
P18	cervical cancer	F	58
P19	colon cancer	M	51
P20	colon cancer	M	55
P21	colon cancer	M	62
P22	colon cancer	F	45
P23	colon cancer	M	61
P24	colon cancer	F	52
P25	breast cancer	F	60
P26	breast cancer	F	55
P27	breast cancer	F	64
P28	breast cancer	F	49
P29	breast cancer	F	57
P30	breast cancer	F	63
P31	breast cancer	F	54
P32	breast cancer (Received PTX+CDDP treatment)	F	71
P33	breast cancer (Received PTX+CDDP treatment)	F	66
P34	breast cancer (Received PTX+CDDP treatment)	F	68

Supplementary Table 2. Comparison of WBCs contamination between our technique and other reported clinical CTCs detection methods.

	Cancer Type	Methods	WBCs contamination
Ref. 1	Prostate cancer	EpCAM targeting	58-9249 per mL
Ref. 2	Non-small cell lung cancer	EpCAM targeting	326 ± 165 per mL
Ref. 3	Breast cancer	EpCAM targeting	350.7 ± 122.8 per 5 mL
Ref. 4	Breast cancer	Physical filtration	663 ± 647 per mL
Our study	Covering 10 cancer types	MGE	341-2750 per mL

509 **References**

510 [S1] Ozkumur, E. et al. (2013). Inertial focusing for tumor antigen-dependent and -independent
511 sorting of rare circulating tumor cells. *Sci. Transl. Med.* ***5***: 179ra47.
512 [S2] Earhart, C. M. et al. (2014). Isolation and mutational analysis of circulating tumor cells
513 from lung cancer patients with magnetic sifters and biochips. *Lab Chip* ***14***: 78.
514 [S3] Cho, H., et al. (2017). A disposable microfluidic device with a reusable magnetophoretic
515 functional substrate for isolation of circulating tumor cells. *Lab Chip* ***17***: 4113.
516 [S4] Lin, E. et al. (2017). High-Throughput Microfluidic Labyrinth for the Label-Free Isolation
517 of Circulating Tumor Cells. *Cell Systems* ***5***: 295.